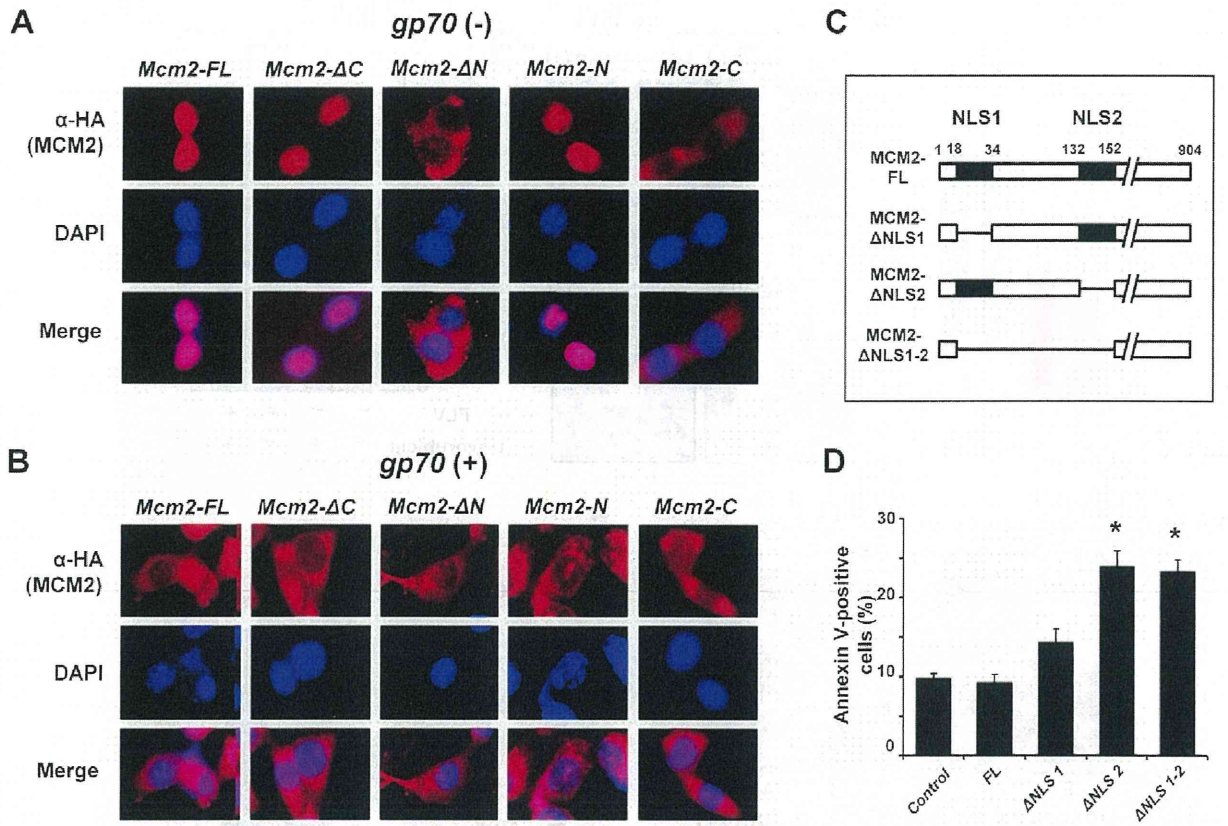

Figure 6. Subcellular localization of MCM2 and the role of the NLS domains in enhancing doxorubicin-induced apoptosis. *HA-Mcm2-FL* and *HA*-mutant-transfected 3T3 cells (**A**), and *FLAG-gp70/HA-Mcm2-FL* and *FLAG-gp70/HA*-mutant-transfected 3T3 cells (**B**) were treated with 1 μM doxorubicin for 24 h. HA-positive cells containing the MCM2-derived proteins are shown in red (TRITC), and DAPI-stained nuclei are shown in blue. Images were acquired using a BZ-9000 microscope (KEYENCE) with a 400× objective. (**C**) Schematic diagram of the NLS deletion mutants MCM2-ΔNLS1, MCM2-ΔNLS2, and MCM2-ΔNLS1-2. (**D**) *Mcm2-NLS* deletion mutant-transfected 3T3 cells were treated with 1 μM doxorubicin for 24 h, and apoptotic cell ratios were determined with annexin V-staining. Data represent the mean and SD of 3 experiments. The asterisks (*) indicate significant differences between the control and *Mcm2-ΔNLS2*- or *Mcm2-ΔNLS 1-2*-transfected cells (*$p<0.01$). Data represent the mean and 95% CI of 3 independent experiments.
doi:10.1371/journal.pone.0040129.g006

these treatments. This is very difficult, but infection with certain types of viruses elicits tumor cell-specific changes in cellular dynamics [48]. Thus, virus-host interaction may provide clues to develop a novel strategy for tumor therapy. Our previous study has shown that FLV infection strongly enhances radiation-induced apoptosis in the hematopoietic cells of C3H mice, although the response is not uniform among the host strains [17]. Elucidation of the molecular mechanisms underlying this host- and cell type-specificity may provide an effective means to induce tumor cell-specific apoptosis in host tissues.

Regarding host specificity, MCM2 was identified as a C3H-specific protein that enhances DNA-damage-induced apoptosis in association with the envelope protein of FLV, gp70. However, MCM2 is part of a conserved set of MCM proteins (MCM2-7), with essential roles in the regulation of DNA replication: functioning as license components for S-phase initiation and further acting as a helicase to unwind DNA at replication forks [25,26,49]. Indeed, MCM proteins are frequently overexpressed in a variety of cancer or pre-cancerous cells [31–36]. In this study, *Mcm2*-transfected 3T3 cells exhibited an increase in proliferation 96 h after transfection. On the other hand, co-transfection of BALB/c-derived 3T3 cells, which originally expressed low levels of *Mcm2*, with *gp70* and *Mcm2* enhanced doxorubicin-induced apoptosis. These results suggest that human tumor cells may also become more sensitive to DNA-damage-induced apoptosis through changes in the molecular functions of MCM2.

MCM2 has several functional domains [50]. However, there are no reports on its functions in apoptosis. Our study demonstrated that a novel functional domain in the C-terminal portion of MCM2 plays a role in apoptosis enhancement under specific conditions in conjunction with gp70 (Figure 8A).

MCM2 is known to interact with various types of molecules, including protein PP2A [51]. PP2A is one of the major Ser/Thr phosphatases implicated in the regulation of cellular processes such as cell cycle progression [52], apoptotic cell death [53–55], and DNA replication and DSB repair [45,52,53]. In the GeneChip assay of the present study, *Ppp2ac* exhibited an expression pattern similar to that of *Mcm2* in the *in vivo* experiments (correlation coefficient >90%; Figure 1L, Table S1). Furthermore, our results suggest that PP2A dephosphorylates DNA-PK and regulates its function, as described previously [44–46]. Depletion of PP2A by RNAi has been shown to induce hyperphosphorylation of DNA-PK and suppression of DNA end-joining followed by enhanced cytogenetic abnormalities including chromosomal and chromatid

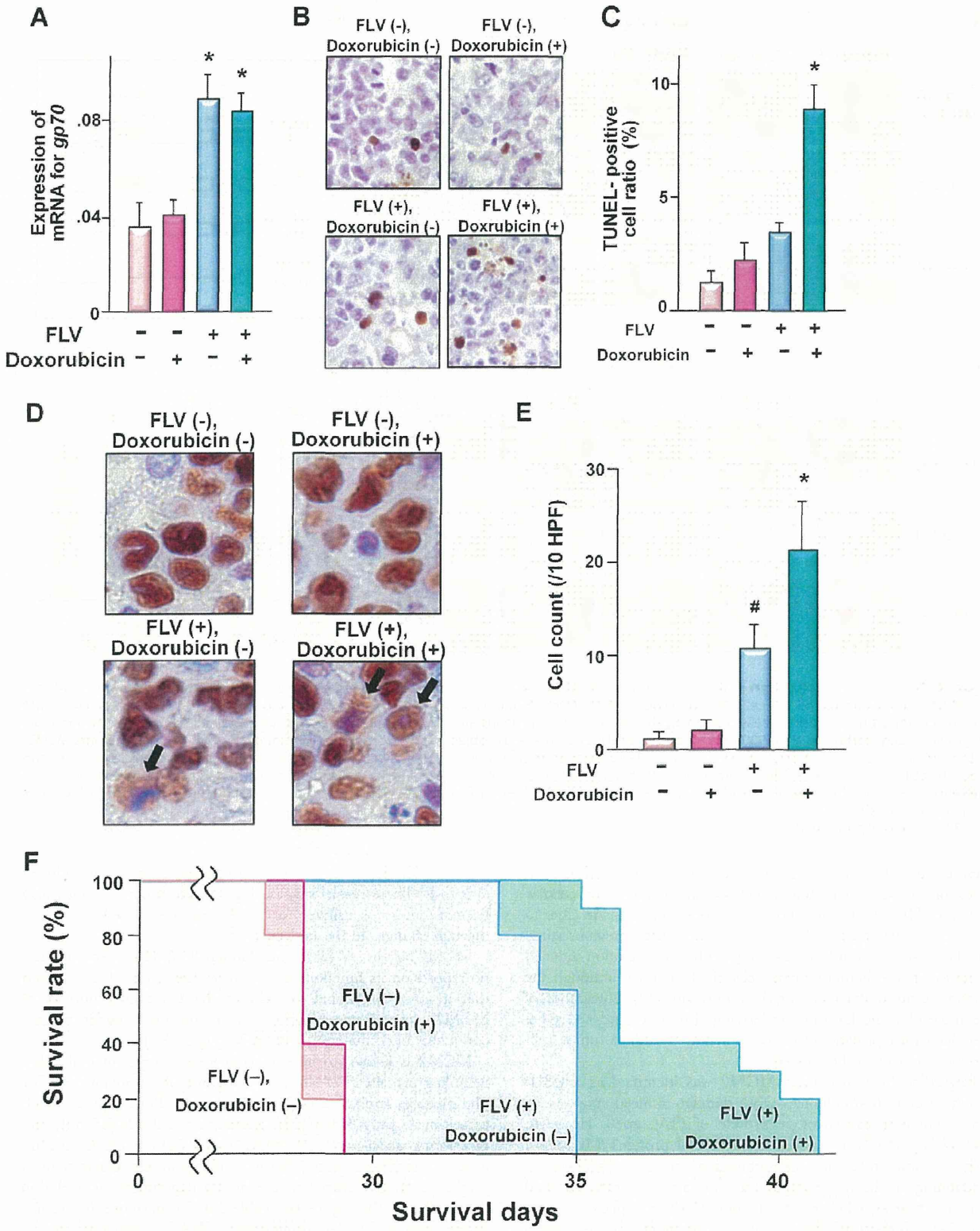

Figure 7. *In vivo* anti-tumor effects of *gp70* expression and DNA-damage on the C3H-derived cells in SCID mice. Two weeks after transplantation, mice were inoculated (i.p.) with FLV. Seven days later, the mice were treated with 1.5 mg/kg of doxorubicin or PBS. (**A**) Quantitative RT-PCR analysis of *gp70* mRNA expression in the liver of SCID mice with multiple foci of leukemic infiltration. The samples from FLV-infected mice

exhibit higher levels of *gp70* than those from uninfected mice (*$p<0.01$). Data represent the mean and 95% CI of from 10 mice in each group and are representative of 2 independent experiments. (**B**) Microscopic features of TUNEL-positive cells in hepatic nodules and (**C**) TUNEL-positive cell ratio in each group of mice. Note the significant increase in apoptotic 8047 cells in mice with FLV infection and doxorubicin treatment (*$p<0.01$ compared with the tumor cells of "FLV (−), doxorubicin (−) mice"). Data represent the mean and 95% CI of from 10 mice in each group and are representative of 2 independent experiments. (**D**) Subcellular localization of MCM2 in 8047 cells of the liver demonstrated by immunohistochemistry. Images were captured with a microscope at 1,000× magnification power. Note the nuclear and/or cytoplasmic localization of MCM2 in the 8047 cells from each group of mice. (**E**) The cell counts for cytoplasmic localization of MCM2. Cell counts are shown as the number of cells per 10 high-power fields (HPF). [# $p<0.01$ compared with tumor cells of "FLV (−), doxorubicin (−)" mice; *$p<0.001$ compared with "FLV (−) doxorubicin (−)" mice and $p<0.05$ compared with "FLV (+), doxorubicin (−)" mice]. Data represent the mean and 95% CI of from 10 mice in each group and are representative of 2 independent experiments. (**F**) Kaplan-Meier survival curves for 8047-transplanted SCID mice with/without FLV-infection and doxorubicin-treatment. Note the significant elongation of survival time in mice with FLV-infection [$p<0.01$ compared with "FLV (−), doxorubicin (−)" and "FLV (−), doxorubicin (+)" mice] and in mice with FLV-infection and doxorubicin-treatment [$p<0.001$ compared with "FLV (−), doxorubicin (−)" and "FLV (−), doxorubicin (+)" mice, $p<0.01$ compared with "FLV (+), doxorubicin (−)" mice]. The survival curves represent data from 10 mice in each group.
doi:10.1371/journal.pone.0040129.g007

breaks [46]. Similar events may result from the interaction of PP2A with MCM2.

The MCM complex (MCM2-7) contains an NLS. MCM2 has 2 NLS domains and histone-binding sites in the N-terminal portion, and therefore deletion of the N-terminal portion resulted in the inhibition of nuclear translocation. NLS2 but not NLS1 is required for the nuclear localization of mouse MCM2 [47]. In the present study, nuclear translocation of MCM2 was inhibited by the binding of gp70 to NLS1, and that the cytoplasmic MCM2 enhanced DNA-damage-induced apoptosis.

In conclusion, we identified a novel function of MCM2: the enhancement of DNA-damage-induced apoptosis. This function occurred in association with gp70, an FLV-derived envelope protein. Gp70 directly bound to the N-terminal portion of MCM2 and inhibited its translocation. The cytoplasmic MCM2-gp70-complex induced an interaction of MCM2 with PP2A, thereby interfering with the PP2A-DNA-PK interaction and leading to enhanced DNA-damage-induced apoptosis via the activation of P53 by DNA-PK (Figure 8B). These results suggest that regulation of the molecular dynamics of MCM2 may be a novel apoptosis-inducing therapeutic method to specifically target malignant tumors that express higher levels of MCM2 than normal tissues.

Materials and Methods

Ethics Statement

Animal experiments were conducted and carried out in strict accordance with the Act on Welfare and Management of Animals of the government of Japan and the Guidelines for the Care and Use of Laboratory Animals of the Tokyo Medical and Dental University. All experiments were approved by the Animal Experiment Committee of the Tokyo Medical and Dental University (No. 100115). All efforts were made to minimize suffering in animal experiments.

Mice and Cell Lines

Eight to 10-week-old male C3H/HeJ mice ($H-2^b$) raised under specific-pathogen-free conditions were purchased from Japan SLC, Inc. (Shizuoka, Japan) with the permission of Dr. Yoshiya Shimada of the National Institute of Radiological Sciences in Chiba. Specific-pathogen-free C57BL/6J mice ($H-2^b$) and BALB/c mice ($H-2^d$) aged 8–10 weeks were also purchased from Japan SLC, Inc. Six-week-old male specific-pathogen-free SCID mice (C.B.17$^{scid/scid}$, $H-2^d$) were purchased from CLEA Japan Inc. (Tokyo, Japan).

The mouse fibroblast cell line 3T3 and the mouse acute myeloid leukemia cell line, BaF3, both derived from BALB/c mice, and the C3H mouse bone marrow cell-derived 32D cells were purchased from the RIKEN Cell Bank (Tsukuba, Ibaraki, Japan). The radiation-induced myeloid leukemia cell line from C3H mice, 8047, was established at the National Institute of Radiological Sciences in Chiba [22]. The cells were cultured in RPMI-1640 medium (Sigma, St. Louis, MO, USA). Primary cultured fibroblasts were derived from the lungs of BALB/c and C3H mice and cultured in DMEM (Sigma). The medium was supplemented with 10% fetal calf serum (FCS), penicillin (50 units/mL) (Invitrogen, Carlsbad, CA, USA), and streptomycin (50 μg/mL) (Invitrogen) and the cells were cultured at 37°C in a humidified atmosphere of 5% CO_2 in air.

Antibodies and Reagents

Rabbit polyclonal anti-glyceraldehyde-3-phosphate dehydrogenase (GAPDH) antibody (Santa Cruz Biotechnology, Santa Cruz, CA, USA), rabbit polyclonal anti-ATM antibody (MILLIPORE, Billerica, MA, USA), mouse monoclonal anti-DNA-PK$_{cs}$ antibody (Santa Cruz), rabbit polyclonal anti-DNA-PK S2056 (Mouse-S2053) antibody (Assay Biotech, Sunnyvale, CA, USA), mouse monoclonal anti-P53 antibody (Merck, Darmstadt, Germany), rabbit polyclonal anti-phospho-P53 (Ser 15) antibody (Merck), rabbit monoclonal anti-cleaved caspase-3 antibody (Cell Signaling Technology [CST], Danvers, MA, USA), rabbit polyclonal anti-MCM3 antibody (CST), mouse monoclonal anti-MCM4 antibody (Santa Cruz Biotechnology), mouse monoclonal anti-HA tag antibody (Invivogen, San Diego, CA, USA), and mouse monoclonal anti-FLAG M2 antibody (Sigma) were used as primary antibodies for immunoblotting. Rabbit polyclonal anti-FLAG antibody (Sigma), rabbit polyclonal anti-HA antibody (Sigma), and rabbit polyclonal anti-PP2A antibody (CST) were used for immunoprecipitation. Horseradish peroxidase (HRP)-conjugated anti-mouse IgG and HRP-conjugated anti-rabbit IgG (GE Healthcare, Little Chalfont Buckinghamshire, England) were used as secondary antibodies for immunoblotting. Doxorubicin hydrochloride (Wako, Tokyo, Japan) was used for DNA-damage induction. NU7026 (Calbiochem, La Jolla, CA, USA) was used to inhibit DNA-PK activity. Okadaic acid (OA; Wako) was used to inhibit PP2A.

Viral Infection and DNA-damage Induction

The NB-tropic FLV complex, originally provided by Dr. C. Friend, was prepared as described previously [56]. Eight- to 10-week-old BALB/c, C57BL/6, and C3H mice were inoculated intraperitoneally (i.p.) with FLV at a highly leukemogenic dose of 10^4 PFU/mouse [57]. On day 7 after the infection with FLV, BALB/c, C57BL/6, and C3H mice were administered (i.p.) with 1.5 mg/kg of doxorubicin hydrochloride. In experiments *in vitro*, 3T3 cells were treated with 1 μM doxorubicin to induce apoptosis.

Detection of Apoptotic Cells

To determine the apoptotic cell ratios in mouse bone marrow and spleen cells after treatment with 1.5 mg/kg of doxorubicin for

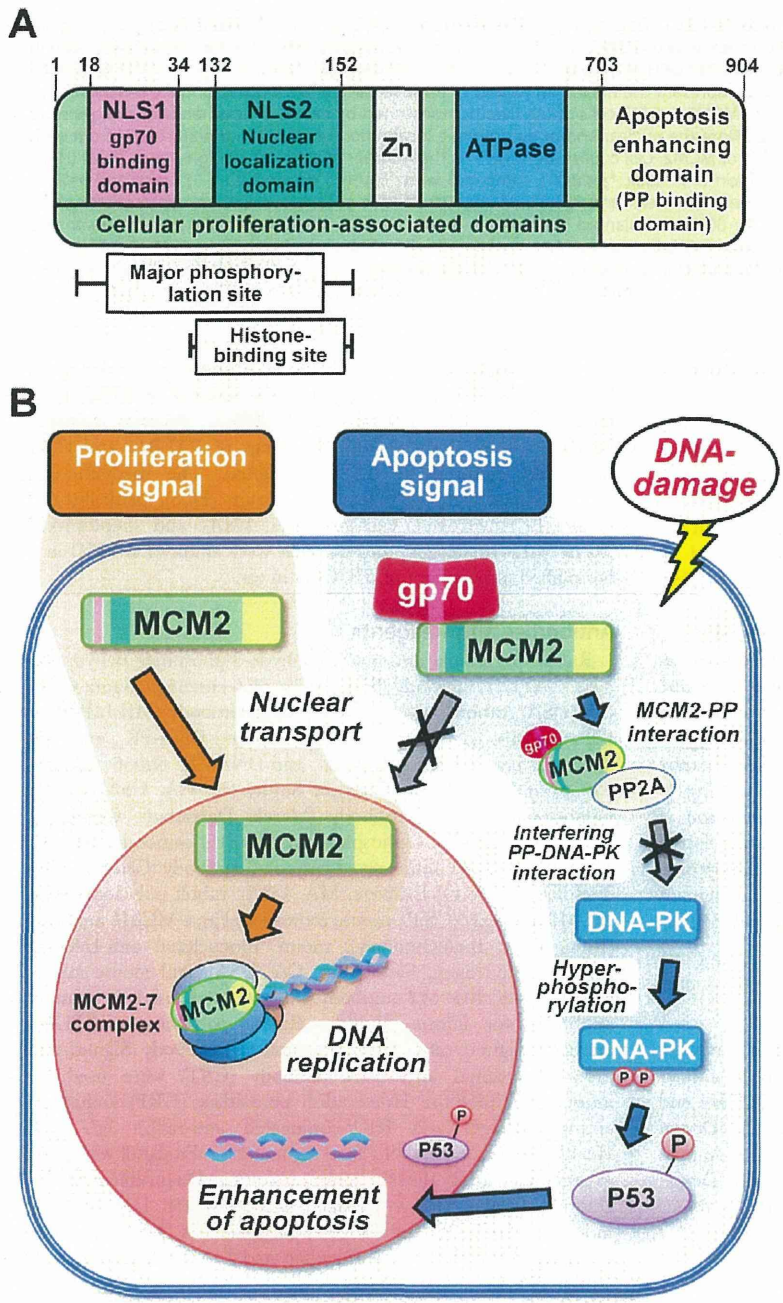

Figure 8. Schematic illustration of the structure of MCM2 and its functions in the cytoplasm and nucleus. (**A**) The various functional domains of the MCM2 protein are shown, and the domains and regions required for the activities are indicated. (**B**) Schematic of the novel role of MCM2 in apoptosis enhancement. Normally, MCM2 is recruited into the nucleus for participation in DNA replication. As a result, cellular proliferation is upregulated (proliferation signal). However, when gp70 is present in the cytoplasm, it binds to MCM2 and inhibits its nuclear entry. Furthermore, cytoplasmic gp70-MCM2-complex interacts with PP2A and inhibits its interaction with DNA-PK. Consequently, hyperphosphorylated DNA-PK enhances DNA-damage-induced apoptosis via a P53-related pathway (apoptosis signal).
doi:10.1371/journal.pone.0040129.g008

24 h, samples were collected from each experimental group, washed with ice-cold PBS, stained with propidium iodide (BD Biosciences, San Jose, CA, USA) and fluorescein isothiocyanate (FITC)-labeled anti-annexin V antibody (BD), and analyzed on a FACScan flow cytometer (BD FACSCanto^{TM} Flow Cytometer).

To determine the apoptotic cell ratios in 32D, BaF3, and 3T3 cells after treatment with 1 μM doxorubicin for 24 h, samples were collected from each experimental group and washed with ice-cold PBS. These samples were stained with propidium iodide (PI), incubated with FITC-labeled anti-annexin V antibody, and

analyzed on a FACScan flow cytometer. For detecting apoptotic cells in tissue sections, the terminal deoxy-transferase (TdT)-mediated dUTP nick-end labeling (TUNEL) method was used as previously described [58]. Briefly, tissue sections were deparaffinized and incubated with proteinase K (prediluted, DAKO Cytomation, Glostrup, Denmark) for 15 min at room temperature. After the tissues were washed, TdT, FITC-dUTP and -dATP (BoehringerMannheim, Mannheim, Germany) were applied and the sections were incubated in a moist chamber for 60 min at 37°C. Anti-FITC-conjugated antibody-peroxidase (POD converter, Boehringer Mannheim) was employed to detect FITC-dUTP labeling, and color development was achieved with 3,3′-diaminobenzidine (DAB) solution containing 0.3% hydrogen peroxide. The sections were then observed under a microscope and the proportion of TUNEL-positive cells was determined by dividing the number of positively stained cells by the total number of cells.

Sybr Green Real-time RT-PCR

RNA was extracted from the bone marrow and spleen cells of BALB/c, C57BL/6, and C3H mice, 8047, 32D, BaF3, and 3T3 cell lines, and primary cultured fibroblasts using Trizol (Invitrogen) according to the manufacturer's instructions. Briefly, the liquid phase was incubated with chloroform for phase separation. Total RNA was finally extracted using one isopropanol precipitation step and one ethanol wash. The RNA pellet was diluted in RNase- and DNase- free water (Qiagen, Hilden, Germany). Then cDNA was generated from RNA using TaqMan® Reverse Transcription Reagents (Applied Biosystems, Foster, CA, USA) and quantitative RT-PCR was performed. For quantitative RT-PCR, specific primers were used with the Lightcycler Sybr Green master mix (Roche, Basel, Switzerland). The sequences of the primers are as follows: for *Mcm2*, GAGGATGGAGAGGAACTCATTG and ATCTTCCTCGCTGCTGTCA; for *Dna-pk*, GAATTCACCACAACCCTGCT and GCTTTCAGCAGGTTCACACA; for *Atm*, CCTTTGTCCTTCGCGATGTTA and GCTGTATGACAAACTCGACTTAATAGGT; and for *gp70*, AAGGTCCAG CGTTCTCAAAAC and AGGTGGCGTTAGCTGTTTGT. The PCR product was detected using the ABI Prism 7900HT Sequence Detection System (Applied Biosystems [ABI], Carlsbad, CA, USA). The primers and TaqMan probes for *Gapdh* were purchased from ABI. *Mcm2*, *Dna-pk*, *Atm*, and *gp70* RNA levels were normalized to that of *Gapdh*.

GeneChip Analysis

FLV-infected or uninfected C57BL/6 and C3H mice were administered (i.p.) with 15 mg/kg (high dose) or 1.5 mg/kg (low dose) of doxorubicin, and the spleen was sampled at 0, 1, 6, and 24 h after administration. Total RNA was isolated using RNeasy mini kit (Qiagen), according to the manufacturer's instructions. First-strand cDNAs were synthesized by incubating 5 μg of total RNA with 200 U of SuperScript II reverse transcriptase (Invitrogen) and 100 pmol of the T7-$(dT)_{24}$ primer [5′-GGCCAGTGAATTGTAATACGACTCACTATAGGGAGGCGG-$(dT)_{24}$-3′]. After second-strand synthesis, the double-stranded cDNAs were purified using a GeneChip Sample Cleanup Module (Affymetrix, Santa Clara, CA, USA), according to the manufacturer's instructions. Double-stranded cDNAs were labeled by *in vitro* transcription using a BioArray High Yield RNA transcript labeling kit (Enzo Diagnostics, Farmingdale, NY, USA). The labeled cRNA was then purified using a GeneChip Sample Cleanup Module (Affymetrix) and treated with 1× fragmentation buffer (40 mM acetate, 100 mM KOAc, 30 mM MgOAc) at 94°C for 35 min. For hybridization to a GeneChip Mouse Genome 430 2.0 Array (Affymetrix), 15 μg of fragmented cRNA probe was incubated with 50 pM control oligonucleotide B2, 1× eukaryotic hybridization control (1.5 pM BioB, 5 pM BioC, 25 pM BioD and 100 pM Cre), 0.1 mg/mL herring sperm DNA, 0.5 mg/mL acetylated BSA and 1× manufacturer-recommended hybridization buffer in a 45°C rotisserie oven for 16 h. Washing and staining were performed with GeneChip Fluidic Station (Affymetrix) using the appropriate antibody dilution, washing and staining protocol. The phycoerythrin-stained arrays were scanned as digital image files and the scanned data were analyzed with GeneChip Operating Software (Affymetrix) [59]. All data are available online (http://www.nihs.go.jp/tox/TtgSubmitted.htm) from the National Institute of Health Sciences.

Transfection of Expression Plasmids

Sequences of full-length mouse MCM2 (MCM2-FL) and MCM2 deletion mutants, MCM2-ΔC (amino acid [aa] 1–703), MCM2-ΔN (aa 156–703), MCM2-N (aa 1–155) and MCM2-C (aa 704–904), were amplified from the cDNA of 8047 cells using PCR primers, and inserted into the *Hind*III/*Xho*I site of the *pcDNA*^{TM}*3.1 3×HA* Expression Vector (Invitrogen). The primers, synthesized at a commercial laboratory (Invitrogen), were as follows: for *Mcm2-FL*, the 5′ primer was GCTCGAGGCGCGGAGTCTTCTGAGTCTCTCTCA and the 3′ primer was ATAAGCTTTCAGAACTGCTGTAGGATCAG; for *Mcm2-ΔC*, GCTCGAGGCGCGGAGTCTTCTGAGTCTCTCTCA and ATAAGCTTTCACTCCAAGGTGCCACCATTA; for *Mcm2-ΔN*, GCTCGAGGCCGCCACAGAGGATGGCGAGGA and ATAAGCTTTCAGAACTGCTGTAGGATCAG; for *Mcm2-N*, GCTCGAGGCGCGGAGTCTTCTGAGTCTCTCTCA and ATAAGCTTTCAGCGTTCTACGTGGCGGCGC; and for *Mcm2-C*, GCTCGAGGCCCAGCCATGCCCAACACATAT and ATAAGCTTTCAGAACTGCTGTAGGATCAG. The sequence encoding viral gp70 protein was amplified from the cDNA of FLV-infected 8047 cells using the PCR primers, and inserted into the *Not*I/*Xba*I site of the *p3×FLAG-CMV*^{TM}*-10* Expression Vector (Sigma). The primers for *gp70* were ATAAGAATGCGGCCGCGAAAGGTCCAGCGTTCTCAAAA and GCTCTAGACTAGCTAGCTATGCAGCTATGCCGCCCATAGT. The *3×HA-Mcm2-ΔNLS1*, *Mcm2-ΔNLS2*, and *Mcm2-ΔNLS1-2* constructs were generated by PCR using a KOD-Plus-Mutagenesis kit (TOYOBO, Tokyo, Japan). The primers, synthesized at a commercial laboratory (Invitrogen), were as follows: for *Mcm2-ΔNLS1*, the 5′ primer was CCGGCGCCGCTGACGGGCAGGGCTA and the 3′ primer was GACGCCCTGACCTCCAGCCCTGGCA; for *Mcm2-ΔNLS2*, GCGCATGCGTCCCAGGCCTCTGCCA and CACGTAGAACGCGCCACAGAGGATG; and for *Mcm2-ΔNLS1-2*, CCGGCGCCGCTGACGGGCAGGGCTA and CACGTAGAACGCGCCACAGAGGATG. The *3×HA-Mcm2*, *Mcm2-ΔC*, *Mcm2-ΔN*, *Mcm2-C*, *Mcm2-N*, *Mcm2-ΔNLS1*, *Mcm2-ΔNLS2*, *Mcm2-ΔNLS1-2*, and/or *3×FLAG-gp70* constructs were transfected into 3T3 cells (2×10^5 cells) using Hily Max Transfection Reagent (Nippon Gene, Tokyo, Japan). The controls were generated by mock-transfection with an empty vector.

Cell Viability Assay

Cell viability was measured using a Cell Proliferation Kit (3-[4,5-dimethylthiazol-2-yl]-2,5-diphenyltetrazolium bromide, MTT) (Roche). Briefly, 3T3 cells were seeded in 96-well plates at 1×10^3/well. After incubation for 24 h, cells were transfected with *3×HA-Mcm2*, *Mcm2-ΔC*, *Mcm2-ΔN*, *Mcm2-C*, *Mcm2-N*, and/or *3×FLAG-gp70*. Twenty-four hours after the transfection, the cells were treated with 1 μM doxorubicin in culture medium for 24 h. Then 10 μL of MTT labeling reagent was added to each well and incubation continued for 4 h at 37°C. Next, 100 μL of

solubilization solution was added to each well and incubation was continued overnight at 37°C. Absorbance was determined at 560 nm using a microplate reader (Bio-Rad, Hercules, CA, USA).

RNA Interference

Small-interfering RNA (siRNA) was used to silence the *Mcm2* gene. The sequence of siRNA used was CAGGTGACAGACTTTATCAAA. An irrelevant siRNA (GCACACAGACTGCAATCACAGGTTA) that did not lead to specific degradation of any cellular mRNA was used as a negative control. BaF3 and 32D cells (2×10^5 cells) were transfected with 120 pmol of *Mcm2* or control siRNA using Amaxa® Cell Line Nucleofector® Kit V (LONZA, Basel, Switzerland) according to the manufacturer's instructions. The oligonucleotides used for cloning short hairpin RNA (shRNA)-encoding sequences targeting DNA-PK and ATM into the pSUPER vector (Oligoengine, Seattle, WA, USA) were as follows: *Sh-Dna-pk*; GATCCCCAGGGCCAAGCTATCATTCTttcaagagaAGAATGATAGCTTGGCCCTTTTTTA; and *sh-Atm*; GATCCCCCATACTAAAGACATTttcaagagaAATGTCTTTGAGTAGTATGTTTTTA. The annealed oligonucleotides were subcloned into *Bgl*II and *Hin*dIII sites. These constructs were transfected into 3T3 cells (2×10^5 cells) using Hily Max Transfection Reagent (Nippon Gene). The controls were generated by mock-transfected with a *sh-empty* vector.

Immunoprecipitation and Immunoblotting

Cell lysates were prepared by incubating cell pellets on ice for 30 min in ice-cold lysis buffer containing 10 mM Tris-HCl, pH 7.5, 5 mM EDTA, 1% Nonidet P-40, 0.02% NaN3, 1 mM PMSF, 0.1% aprotinin, 100 μM leupeptin and 100 μM TPCK (Sigma). Cell lysates were incubated with antibody and Protein G Sepharose™ (GE Healthcare). The immunoprecipitates obtained after centrifugation or whole cell lysates were mixed with 2× sodium dodecyl sulfate (SDS) buffer (125 mM Tris-HCl at pH 6.8, 4% SDS, 20% glycerol, 0.01% bromophenol blue, and 10% 2-mercaptoethanol) and boiled for 10 min. The samples were loaded onto a 5–20% or 3–10% gradient polyacrylamide gel (WAKO), and electrophoretically transferred to nitrocellulose membranes (GE Healthcare). The membranes were blocked with 10% skim milk in PBS, incubated with primary antibodies, washed, and incubated with peroxidase-conjugated secondary antibodies. The protein signal was detected using the ECL Plus Western Blotting Detection System (GE Healthcare).

Chromatin Loading Assay

Chromatin loading of MCM2 was performed as described previously [60]. Briefly, 3T3 cells were harvested using trypsin, and the cell pellets were lysed by incubating in complete cytoskeleton (CSK) buffer (20 mM HEPES, 100 mM NaCl, 3 mM $MgCl_2$, 300 mM sucrose, and 0.1% NP-40) for 15 min on ice. Cytoplasmic fractions were obtained as supernatants after low speed centrifugation (3,000×g) at 4°C. Pellets were rinsed with complete CSK buffer for 10 min on ice and recentrifuged to obtain a chromatin-enriched fraction. Pellets were then sonicated for 5 s in CSK buffer and subjected to high-speed centrifugation (16,000×g). The post-sonication supernatant was designated as the chromatin-bound fraction.

Analysis of Cell Cycle Distribution

Cell cycle distribution was monitored by quantifying the cellular DNA content after staining with PI. Cells were fixed with ethanol for 20 min at −20°C. After centrifugation, cells were suspended in PBS containing PI (50 μg/mL) and RNase (0.2 mg/mL), incubated at room temperature for 30 min, and analyzed on a FACScan flow cytometer (BD FACSCanto™ Flow Cytometer).

Immunofluorescence

3T3 cells were fixed in 1% paraformaldehyde in PBS and permeabilized with 0.1% NP-40 in PBS at room temperature. Cells were incubated with mouse monoclonal anti-HA antibody (Invivogen) at a 1:100 dilution in PBS for 1 h at room temperature. Cells were then stained with tetramethylrhodamine-5-(and 6)-isothiocyanate (TRITC)-conjugated anti-rabbit antibody (Dako Cytomation, Glostrup, Denmark) at a 1:100 dilution for 20 min at room temperature. Slides were washed 3 times with PBS and mounted with Vectashield mounting medium containing 4′,6-diamidino-2-phenylindole (DAPI; Vector Laboratories, Inc., Burlingame, CA, USA). Images were acquired using a BZ-9000 microscope (KEYENCE, Osaka, Japan) with a 400× objective.

Transplantation of MCM2-expressing Leukemia Cells into SCID Mice and Apoptosis Induction

The 8047 cells (1 x 10^5 cells) derived from C3H mice were transplanted intravenously into SCID mice via the tail vein. Two weeks after the transplantation, FLV was injected (i.p.) into SCID mice at a dose of 10^4 PFU/mouse. Then, 7 days after FLV inoculation, the mice were treated twice a week with 1.5 mg/kg of doxorubicin.

Immunohistochemistry

Formalin-fixed paraffin-embedded tissue sections (4 μm thick) of the liver from 8047-transplanted SCID mice were de-waxed in xylene and re-hydrated through graded alcohol to water. Antigen retrieval was achieved with a 10-min autoclave treatment in 0.1 M citrate buffer (pH6.0). Endogeneous peroxidase activity was inhibited by dipping the slides in 0.3% hydrogen peroxide in methanol for 30 min and non-specific protein binding was blocked by incubation with normal horse serum (Vector Laboratories, Burlingame, CA, USA). Sections were then treated with anti-MCM2 mouse monoclonal antibody (BD Biosciences) (1:2,000) overnight at 4°C. Detection was achieved using the streptavidin-biotin-peroxidase complex technique (Vector Laboratories) with DAB as the chromogen.

Statistical Analysis

Statistical significance was determined using a two-tailed Student's *t*-test. For Kaplan-Meier analysis of SCID mice transplanted with 8047 cells, a log-rank test was performed.

Supporting Information

Figure S1 Gp70 suppresses the formation of the MCM complex. Control, *HA-Mcm2*-transfected and *HA-Mcm2/FLAG-gp70*-transfected 3T3 cells were left untreated or treated with 1 μM doxorubicin for 24 h. Cell lysates were subjected to a pull-down assay to detect the binding of MCM3 or MCM4 to HA-MCM2. In *Mcm2*-transfected 3T3 cells, MCM2 interacts with MCM3 and MCM4, both in the presence and absence of doxorubicin-treatment. By contrast, in *gp70* plus *Mcm2*-transfected 3T3 cells, MCM2 does not co-precipitate with MCM3 or MCM4 after treatment with doxorubicin. These results suggest that gp70 binds to MCM2 and inhibits the formation of the MCM complex and the binding to chromatin under DNA-damage by doxorubicin.
(TIF)

Figure S2 Gp70 directly interacts with MCM2. (**A**) Schematic diagram of full-length gp70 (gp70-FL) and the gp70 deletion mutants, gp70-1 (aa 1–153), gp70-2 (aa 154–330), and gp70-3 (aa 331–461). 3T3 cells were transfected with *FLAG*-tagged *gp70* mutants along with *HA*-tagged *Mcm2* and left untreated (**B**) or treated with 1 μM doxorubicin for 24 h (**C**). The expression of the gp70 mutants (**B**, **C**, left upper) and HA-MCM2 (**B**, **C**, left middle) was confirmed in 3T3 cells. Cell lysates were subjected to a pull-down assay to detect the binding of gp70-FL or the mutants to HA-MCM2 (**B**, **C**, right panel). Apoptotic cell ratios were determined with annexin V-staining of *Mcm2-FL/gp70* mutant-transfected 3T3 cells that were left untreated (**D**) or treated with 1 μM doxorubicin for 24 h (**E**). Asterisks (*) indicate significant differences between mutant-transfected cells and the control ($p<0.01$). Data represent the mean and 95% CI of 3 independent experiments.
(TIF)

Figure S3 Effects of MCM2 and deletion mutant overexpression on 3T3 cell proliferation. 3T3 cells were transfected with *Mcm2-FL* or the *Mcm2* deletion mutants and the cell number was counted at an early phase (48 h, **A**, **B**) and a late phase (96 h, **C**, **D**) after transfection with (**A**, **C**) or without (**B**, **D**) *gp70*. Data represent the mean and 95% CI of 3 independent experiments. Note the significant increase in cell counts following *Mcm2-FL-* and *Mcm2-* ΔC-transfection (*$p<0.01$).
(TIF)

Figure S4 Knockdowns of *Dna-pk* and *Atm* in *gp70* plus *Mcm2*-transfected cells using the pSUPER shRNA system. The expression of *Dna-pk* (**A**) and *Atm* (**B**) mRNAs and DNA-PK (**C**) and ATM (**D**) proteins were examined by quantitative RT-PCR and western blotting, respectively. Cell survival (**E**, **G**) and apoptotic cell ratio (**F**, **H**) were determined with the MTT assay and annexin V-staining, respectively, after treatment with 1 μM doxorubicin for 24 h. Note the apoptosis-abrogating effects of *sh-Dna-pk* (**E**, **F**). Asterisks (*) indicate significant differences between *sh-Dna-pk*-treated and *sh-Control*-treated cells (*$p<0.01$). However, *Atm* knockdown causes no remarkable change in viability or apoptotic cell ratio relative to that of cells treated with *sh-Control* (**G**, **H**). Data represent the mean and 95% CI of 3 independent experiments.
(TIF)

Figure S5 Effects of MCM2 and deletion mutant overexpression on the cell-cycle distribution of 3T3 cells. 3T3 cells were transfected with the *Mcm2* deletion mutants with (**A**) or without (**B**) *gp70* and treated with 1 μM doxorubicin for 24 h. The cells were fixed with ethanol, stained with propidium iodide (PI), and analyzed by flow cytometry. Data represent the mean and 95% CI of 3 independent experiments. 3T3 cells exhibit an increase in G2/M fraction after treatment with doxorubicin. However, the differences between the cell cycle profiles of *Mcm-2* or *gp70-* transfected cells are not significant.
(TIF)

Figure S6 Co-localization of gp70, MCM2, and DNA-PK in the cytoplasmic fraction of 3T3 cells. Control, *HA-Mcm2*-transfected and *HA-Mcm2/FLAG-gp70*-transfected 3T3 cells were left untreated (left) or treated with 1 μM doxorubicin for 24 h (right). Cell lysates from these cells were separated into chromatin-bound and cytoplasmic fractions. HA-MCM2 (upper) and DNA-PK (bottom) were detected by western blotting. In *Mcm2*-transfected 3T3 cells, MCM2 binds to the chromatin irrespective of doxorubicin treatment. By contrast, in *gp70* plus *Mcm2*-transfected 3T3 cells, MCM2 does not bind to the chromatin after treatment with doxorubicin (upper). DNA-PK is not detected in the chromatin-bound and cytoplasmic fractions of samples not treated with doxorubicin. Under doxorubicin-treated conditions, equal proportions of chromatin-bound DNA-PK are seen in all groups. By contrast, DNA-PK is more strongly expressed in the cytoplasmic fraction of *gp70* plus *Mcm2*-transfected 3T3 cells than in the other groups (bottom). These results suggest that gp70, MCM2, and DNA-PK co-localize in the cytoplasm, leading to subsequent P53 activation and apoptosis induction.
(TIF)

Figure S7 Subcellular localization and interactions of MCM2 NLS deletion mutants in 3T3 cells. (**A**) 3T3 cells transfected with *HA*-tagged *Mcm2 NLS* deletion mutants were treated with 1 μM doxorubicin for 24 h. The cells were then fixed with 1% paraformaldehyde in PBS, permeabilized with 0.1% NP-40 in PBS at room temperature, and stained with TRITC-conjugated anti-HA antibody. HA-positive cells are shown in red (TRITC), and DAPI-stained nuclei are shown in blue. Images were acquired using a BZ-9000 microscope (KEYENCE) with a 400× objective. Note the nuclear localization of MCM2-ΔNLS1 in contrast to the cytoplasmic localization of MCM2-ΔNLS2 and MCM2-ΔNLS1-2. (**B**) 3T3 cells were transfected with *HA*-tagged *Mcm2 NLS* deletion mutants along with *FLAG*-tagged *gp70*, and treated with 1 μM doxorubicin for 24 h. Expression of the MCM2 NLS deletion mutants (left panel, upper) and FLAG-gp70 (left panel, middle) was confirmed by western blotting. Lysates from these cells were subjected to a pull-down assay to detect the binding of the MCM2 NLS deletion mutants to FLAG-gp70. MCM2-FL and MCM2-ΔNLS2 proteins coprecipitate with gp70 (right panel). Thus, gp70 is able to interact with MCM2-FL and MCM2-ΔNLS2, but not with MCM2-ΔNLS1 or MCM2-ΔNLS1-2. These results suggest that gp70 is bound to the NLS1 domain of MCM2 and indirectly inhibits the function of NLS2.
(TIF)

Table S1 Identification of genes with expression patterns similar to that of *Mcm2* using the GeneChip assay. Gene expression patterns were determined by the GeneChip assay in FLV-infected or un-infected C3H/C57BL/6 mice after treatment with doxorubicin. A part of genes exhibited similar expression patterns with *Mcm2*. The similarity in gene expression patterns was evaluated with the Percellome system using a Pearson product-moment correlation coefficient.
(DOCX)

Acknowledgments

We thank Ms. Sachiko Ishibashi of the Tokyo Medical and Dental University for technical assistance.

Author Contributions

Conceived and designed the experiments: SA M. Kitagawa M. Kurata. Performed the experiments: SA M. Kurata SS KY. Analyzed the data: SA M. Kurata. Contributed reagents/materials/analysis tools: KA JK. Wrote the paper: SA M. Kitagawa.

References

1. Kruse JP, Gu W (2009) Modes of p53 regulation. Cell 137: 609–622.
2. Zhou BB, Elledge SJ (2000) The DNA damage response: putting checkpoints in perspective. Nature 408: 433–439.
3. Batchelor E, Mock CS, Bhan I, Loewer A, Lahav G (2008) Recurrent initiation: a mechanism for triggering p53 pulses in response to DNA damage. Mol Cell 30: 277–289.

4. Gudkov AV, Komarova EA (2003) The role of p53 in determining sensitivity to radiotherapy. Nat Rev Cancer 3: 117–129.
5. Myers JS, Cortez D (2006) Rapid activation of ATR by ionizing radiation requires ATM and Mre11. J Biol Chem 281: 9346–9350.
6. Brady CA, Jiang D, Mello SS, Johnson TM, Jarvis LA, et al. (2011) Distinct p53 transcriptional programs dictate acute DNA-damage responses and tumor suppression. Cell 145: 571–583.
7. Kennedy AL, McBryan T, Enders GH, Johnson FB, Zhang R, et al. (2010) Senescent mouse cells fail to overtly regulate the HIRA histone chaperone and do not form robust Senescence Associated Heterochromatin Foci. Cell Div 5: 16.
8. Barlow C, Brown KD, Deng CX, Tagle DA, Wynshaw-Boris A (1997) Atm selectively regulates distinct p53-dependent cell-cycle checkpoint and apoptotic pathways. Nat Genet 17: 453–456.
9. Harper JW, Elledge SJ (2007) The DNA damage response: ten years after. Mol Cell 28: 739–745.
10. Bakkenist CJ, Kastan MB (2003) DNA damage activates ATM through intermolecular autophosphorylation and dimer dissociation. Nature 421: 499–506.
11. Shiloh Y (2003) ATM and related protein kinases: safeguarding genome integrity. Nat Rev Cancer 3: 155–168.
12. Woo RA, Jack MT, Xu Y, Burma S, Chen DJ, et al. (2002) DNA damage-induced apoptosis requires the DNA-dependent protein kinase, and is mediated by the latent population of p53. EMBO J 21: 3000–3008.
13. Kaelin WG Jr (1999) The emerging p53 gene family. J Natl Cancer Inst 91: 594–598.
14. Adeyemi RO, Landry S, Davis ME, Weitzman MD, Pintel DJ (2010) Parvovirus minute virus of mice induces a DNA damage response that facilitates viral replication. PLoS Pathog 6: e1001141.
15. Feng P, Liang C, Shin YC, Xiaofei E, Zhang W, et al. (2007) A novel inhibitory mechanism of mitochondrion-dependent apoptosis by a herpesviral protein. PLoS Pathog 3: e174.
16. Qian Z, Leung-Pineda V, Xuan B, Piwnica-Worms H, Yu D (2010) Human cytomegalovirus protein pUL117 targets the mini-chromosome maintenance complex and suppresses cellular DNA synthesis. PLoS Pathog 6: e1000814.
17. Kitagawa M, Yamaguchi S, Hasegawa M, Tanaka K, Sado T, et al. (2002) Friend leukemia virus infection enhances DNA damage-induced apoptosis of hematopoietic cells, causing lethal anemia in C3H hosts. J Virol 76: 7790–7798.
18. Banin S, Moyal L, Shieh S, Taya Y, Anderson CW, et al. (1998) Enhanced phosphorylation of p53 by ATM in response to DNA damage. Science 281: 1674–1677.
19. Hasegawa M, Yamaguchi S, Aizawa S, Ikeda H, Tatsumi K, et al. (2005) Resistance against Friend leukemia virus-induced leukemogenesis in DNA-dependent protein kinase (DNA-PK)-deficient scid mice associated with defective viral integration at the Spi-1 and Fli-1 site. Leuk Res 29: 933–942.
20. Yamaguchi S, Hasegawa M, Aizawa S, Tanaka K, Yoshida K, et al. (2005) DNA-dependent protein kinase enhances DNA damage-induced apoptosis in association with Friend gp70. Leuk Res 29: 307–316.
21. Tanaka K, Watanabe K, Yamaguchi S, Hasegawa M, Kitagawa M, et al. (2004) Cytological basis for enhancement of radiation-induced mortality by Friend leukaemia virus infection. Int J Radiat Biol 80: 673–681.
22. Hasegawa M, Kurata M, Yamamoto K, Yoshida K, Aizawa S, et al. (2009) A novel role for acinus and MCM2 as host-specific signaling enhancers of DNA-damage-induced apoptosis in association with viral protein gp70. Leuk Res 33: 1100–1107.
23. Bochman ML, Schwacha A (2008) The Mcm2–7 complex has in vitro helicase activity. Mol Cell 31: 287–293.
24. Wu PY, Nurse P (2009) Establishing the program of origin firing during S phase in fission Yeast. Cell 136: 852–864.
25. Maiorano D, Lutzmann M, Mechali M (2006) MCM proteins and DNA replication. Curr Opin Cell Biol 18: 130–136.
26. Tachibana KE, Gonzalez MA, Coleman N (2005) Cell-cycle-dependent regulation of DNA replication and its relevance to cancer pathology. J Pathol 205: 123–129.
27. Liku ME, Nguyen VQ, Rosales AW, Irie K, Li JJ (2005) CDK phosphorylation of a novel NLS-NES module distributed between two subunits of the Mcm2–7 complex prevents chromosomal rereplication. Mol Biol Cell 16: 5026–5039.
28. Nguyen VQ, Co C, Irie K, Li JJ (2000) Clb/Cdc28 kinases promote nuclear export of the replication initiator proteins Mcm2–7. Curr Biol 10: 195–205.
29. Labib K, Kearsey SE, Diffley JF (2001) MCM2–7 proteins are essential components of prereplicative complexes that accumulate cooperatively in the nucleus during G1-phase and are required to establish, but not maintain, the S-phase checkpoint. Mol Biol Cell 12: 3658–3667.
30. Madine MA, Swietlik M, Pelizon C, Romanowski P, Mills AD, et al. (2000) The roles of the MCM, ORC, and Cdc6 proteins in determining the replication competence of chromatin in quiescent cells. J Struct Biol 129: 198–210.
31. Freeman A, Morris LS, Mills AD, Stoeber K, Laskey RA, et al. (1999) Minichromosome maintenance proteins as biological markers of dysplasia and malignancy. Clin Cancer Res 5: 2121–2132.
32. Meng MV, Grossfeld GD, Williams GH, Dilworth S, Stoeber K, et al. (2001) Minichromosome maintenance protein 2 expression in prostate: characterization and association with outcome after therapy for cancer. Clin Cancer Res 7: 2712–2718.
33. Dudderidge TJ, Stoeber K, Loddo M, Atkinson G, Fanshawe T, et al. (2005) Mcm2, Geminin, and KI67 define proliferative state and are prognostic markers in renal cell carcinoma. Clin Cancer Res 11: 2510–2517.
34. Going JJ, Keith WN, Neilson L, Stoeber K, Stuart RC, et al. (2002) Aberrant expression of minichromosome maintenance proteins 2 and 5, and Ki-67 in dysplastic squamous oesophageal epithelium and Barrett's mucosa. Gut 50: 373–377.
35. Davies RJ, Freeman A, Morris LS, Bingham S, Dilworth S, et al. (2002) Analysis of minichromosome maintenance proteins as a novel method for detection of colorectal cancer in stool. Lancet 359: 1917–1919.
36. Majid S, Dar AA, Saini S, Chen Y, Shahryari V, et al. (2010) Regulation of minichromosome maintenance gene family by microRNA-1296 and genistein in prostate cancer. Cancer Res 70: 2809–2818.
37. Greenberger JS, Sakakeeny MA, Humphries RK, Eaves CJ, Eckner RJ (1983) Demonstration of permanent factor-dependent multipotential (erythroid/neutrophil/basophil) hematopoietic progenitor cell lines. Proc Natl Acad Sci U S A 80: 2931–2935.
38. Tenca P, Brotherton D, Montagnoli A, Rainoldi S, Albanese C, et al. (2007) Cdc7 is an active kinase in human cancer cells undergoing replication stress. J Biol Chem 282: 208–215.
39. Zegerman P, Diffley JF (2010) Checkpoint-dependent inhibition of DNA replication initiation by Sld3 and Dbf4 phosphorylation. Nature 467: 474–478.
40. Montagnoli A, Valsasina B, Brotherton D, Troiani S, Rainoldi S, et al. (2006) Identification of Mcm2 phosphorylation sites by S-phase-regulating kinases. J Biol Chem 281: 10281–10290.
41. Lau KM, Chan QK, Pang JC, Li KK, Yeung WW, et al. (2010) Minichromosome maintenance proteins 2, 3 and 7 in medulloblastoma: overexpression and involvement in regulation of cell migration and invasion. Oncogene 29: 5475–5489.
42. Mukherjee B, Kessinger C, Kobayashi J, Chen BP, Chen DJ, et al. (2006) DNA-PK phosphorylates histone H2AX during apoptotic DNA fragmentation in mammalian cells. DNA Repair (Amst) 5: 575–590.
43. Neal JA, Meek K (2011) Choosing the right path: does DNA-PK help make the decision? Mutat Res 711: 73–86.
44. Douglas P, Moorhead GB, Ye R, Lees-Miller SP (2001) Protein phosphatases regulate DNA-dependent protein kinase activity. J Biol Chem 276: 18992–18998.
45. Chowdhury D, Keogh MC, Ishii H, Peterson CL, Buratowski S, et al. (2005) gamma-H2AX dephosphorylation by protein phosphatase 2A facilitates DNA double-strand break repair. Mol Cell 20: 801–809.
46. Wang Q, Gao F, Wang T, Flagg T, Deng X (2009) A nonhomologous end-joining pathway is required for protein phosphatase 2A promotion of DNA double-strand break repair. Neoplasia 11: 1012–1021.
47. Ishimi Y, Komamura Y, You Z, Kimura H (1998) Biochemical function of mouse minichromosome maintenance 2 protein. J Biol Chem 273: 8369–8375.
48. Kanai R, Rabkin SD, Yip S, Sgubin D, Zaupa CM, et al. (2012) Oncolytic virus-mediated manipulation of DNA damage responses: synergy with chemotherapy in killing glioblastoma stem cells. J Natl Cancer Inst 104: 42–55.
49. Bell SP, Dutta A (2002) DNA replication in eukaryotic cells. Annu Rev Biochem 71: 333–374.
50. Ishimi Y, Komamura-Kohno Y, Arai K, Masai H (2001) Biochemical activities associated with mouse Mcm2 protein. J Biol Chem 276: 42744–42752.
51. Dehde S, Rohaly G, Schub O, Nasheuer HP, Bohn W, et al. (2001) Two immunologically distinct human DNA polymerase alpha-primase subpopulations are involved in cellular DNA replication. Mol Cell Biol 21: 2581–2593.
52. Janssens V, Goris J, Van Hoof C (2005) PP2A: the expected tumor suppressor. Curr Opin Genet Dev 15: 34–41.
53. Garcia A, Cayla X, Guergnon J, Dessauge F, Hospital V, et al. (2003) Serine/threonine protein phosphatases PP1 and PP2A are key players in apoptosis. Biochimie 85: 721–726.
54. Li HH, Cai X, Shouse GP, Piluso LG, Liu X (2007) A specific PP2A regulatory subunit, B56gamma, mediates DNA damage-induced dephosphorylation of p53 at Thr55. EMBO J 26: 402–411.
55. Goodarzi AA, Jonnalagadda JC, Douglas P, Young D, Ye R, et al. (2004) Autophosphorylation of ataxia-telangiectasia mutated is regulated by protein phosphatase 2A. EMBO J 23: 4451–4461.
56. Kitagawa M, Matsubara O, Kasuga T (1986) Dynamics of lymphocytic subpopulations in Friend leukemia virus-induced leukemia. Cancer Res 46: 3034–3039.
57. Kitagawa M, Aizawa S, Kamisaku H, Ikeda H, Hirokawa K, et al. (1995) Cell-free transmission of Fv-4 resistance gene product controlling Friend leukemia virus-induced leukemogenesis: a unique mechanism for interference with viral infection. Blood 86: 1557–1563.
58. Kitagawa M, Yamaguchi S, Takahashi M, Tanizawa T, Hirokawa K, et al. (1998) Localization of Fas and Fas ligand in bone marrow cells demonstrating myelodysplasia. Leukemia 12: 486–492.
59. Kanno J, Aisaki K, Igarashi K, Nakatsu N, Ono A, et al. (2006) "Per cell" normalization method for mRNA measurement by quantitative PCR and microarrays. BMC Genomics 7: 64.
60. Chuang LC, Teixeira LK, Wohlschlegel JA, Henze M, Yates JR, et al. (2009) Phosphorylation of Mcm2 by Cdc7 promotes pre-replication complex assembly during cell-cycle re-entry. Mol Cell 35: 206–216.

Molecular and Cellular Endocrinology 362 (2012) 39–47

Contents lists available at SciVerse ScienceDirect

Molecular and Cellular Endocrinology

journal homepage: www.elsevier.com/locate/mce

The aryl hydrocarbon receptor ligands 2,3,7,8-tetrachlorodibenzo-*p*-dioxin and 3-methylcholanthrene regulate distinct genetic networks ☆

Elin Swedenborg [a], Maria Kotka [a], Martin Seifert [b], Jun Kanno [c], Ingemar Pongratz [a], Joëlle Rüegg [d,*]

[a] Department of Biosciences and Nutrition, Karolinska Institutet, Hälsovägen 7, 141 83 Huddinge, Sweden
[b] Genomatix Software GmbH, Bayerstr. 85a, 80335 Munich, Germany
[c] Cellular & Molecular Toxicology Division, Biological Safety Research Center, National Institute of Health Sciences, Kamiyoga 1-18-1, Setagaya-ku, Tokyo 158-8501, Japan
[d] Department of Biomedicine, University of Basel, Mattenstrasse 28, 4058 Basel, Switzerland

ARTICLE INFO

Article history:
Received 21 February 2012
Received in revised form 11 April 2012
Accepted 16 May 2012
Available online 24 May 2012

Keywords:
3-Methylcholanthrene
Dioxin
Estrogen receptor
Arylhydrocarbon receptor
Endocrine disruption

ABSTRACT

The two estrogen receptor isoforms ERα and ERβ mediate biological effects of estrogens, but are also targets for endocrine disruptive chemicals (EDCs), compounds that interfere with hormonal signaling. 3-Methylcholanthrene (3-MC) and dioxin (TCDD) are EDCs and prototypical aryl hydrocarbon receptor (AhR) agonists, and can inhibit ER signaling. However, in contrast to TCDD, 3-MC gives rise to metabolites with estrogenic properties.

We compared gene expression profiles in HepG2 cells after exposure to 3-MC, TCDD, and the synthetic estrogen diethylstilbestrol (DES). Interestingly, we observed little overlap between the genetic networks activated by 3-MC and TCDD, two compounds sometimes considered as interchangeable AhR ligands. Like DES, 3-MC induced a number of ER-regulated genes and lead to recruitment of ERα to the promoters of such genes. Interestingly, in contrast to DES, the estrogenic effects exerted by 3-MC were exclusively observed in ERα, but not in ERβ-expressing cells, suggesting ER isoform selectivity of 3-MC-derived metabolites.

1. Introduction

The intensive use of chemicals in modern society has resulted in a plethora of compounds released into the environment. Many of these chemicals disturb hormonal signaling, and are collectively known as endocrine disruptors (EDCs; reviewed in e.g. Ruegg et al., 2009). Exposure to EDCs has raised considerable concern in recent years, and they are implicated in many of the main ailments of the Western societies such as reproductive disturbances (e.g. Vidaeff and Sever, 2005), hormone-related cancers (Mukherjee et al., 2006; Nomura, 2008), and metabolic disorders like obesity and diabetes (reviewed in e.g. Elobeid and Allison, 2008; Newbold et al., 2008; Swedenborg et al., 2009). The molecular basis of endocrine disruption is complex, and the outcome is influenced by many parameters such as exposure dose, developmental stage at time of exposure, and species- and tissue-specific factors.

A system that is particularly vulnerable to EDCs is the estrogen system. The effects of the female sex hormone estrogen are mainly mediated by the estrogen receptors (ERs). There are two main ER isoforms, ERα and ERβ, that have overlapping but not identical functions. The ERs belong to the family of nuclear receptors and are ligand-induced transcription factors. Xenobiotics that affect the estrogen system include dietary substances like phytoestrogens and chemical pollutants such as bisphenols and polyaromatic hydrocarbons (Nilsson et al., 2001). Many of these compounds mediate their action by occupying the ER ligand-binding pocket and thus acting as *bona fide* ligands for one or both ER isoforms, whereas others activate alternative signaling pathways, which in turn interfere with ER biological function.

An example for the latter mechanism is the effect of the environmental pollutant dioxin that interferes with ER signaling but does not bind to the ERs. The most potent dioxin congener, TCDD (2,3,7,8-tetrachlorodibenzo-*p*-dioxin), is formed through incomplete combustion of waste material, e.g. backyard burning of household waste, or as a side product in certain industrial processes. Dioxin is resistant to biodegradation and ubiquitously

Abbreviations: 3-MC, 3-methylcholanthrene; AhR, aryl hydrocarbon receptor; ARNT, AhR nuclear translocator; ChIP, chromatin immunoprecipitation; CYP1A1, cytrochrome P450 1A1; DES, diethylstilbestrol; EDC, endocrine disruptive chemical; ER, estrogen receptor; ERE, estrogen response element; FST, follistatin; GREB-1, growth regulation by estrogen in breast cancer 1; IGFBP4, Insulin-like growth factor binding protein 4; PAI-1, plasminogen activator inhibitor-1/Serpine I; TCDD, 2,3,7,8-tetrachlorodibenzo-*p*-dioxin; TFF1, trefoil factor 1; UTRN, utrophin; XRE, xenobiotic response element.

☆ The authors are supported by the European Commission funded CRESCENDO Integrated Project, the Swiss National Research Foundation, and the Magnus Bergvall Foundation.

* Corresponding author. Tel.: +41 61 695 30 60; fax: +41 61 267 35 66.
E-mail address: Joelle.rueegg@unibas.ch (J. Rüegg).

0303-7207/$ - see front matter © 2012 Elsevier Ireland Ltd. All rights reserved.
http://dx.doi.org/10.1016/j.mce.2012.05.006

present in the environment. The biological responses to dioxin include toxic and teratogenic effects and a marked up-regulation of drug-metabolizing enzymes such as cytochrome P450 1A1 (CYP1A1) (Poland and Knutson, 1982). The biological responses to dioxin are mediated through the aryl hydrocarbon receptor (AhR), an intracellular receptor that binds to many xenobiotic compounds with high affinity. Several molecular mechanisms behind inhibitory AhR-ER crosstalk and anti-estrogenic effects by dioxin have been proposed, such as competition for common cofactors, binding site hindrance and alterations of hormone metabolism (Astroff and Safe, 1990; Boverhof et al., 2008; Chaloupka et al., 1992; Harper et al., 1994; Kharat and Saatcioglu, 1996; Klinge et al., 2000; Ruegg et al., 2008; Zacharewski et al., 1994). The interference might consist of the combination of several mechanisms, depending on cell- and gene-specific factors.

The polycyclic aromatic hydrocarbon (PAH) 3-methylcholanthrene (3-MC) is classified as a human carcinogen. It has been frequently used as a mutagen in cancer studies, due to its ability to form bulky adducts on DNA and thereby cause mutations. It is also considered a classical AhR agonist and CYP1A1 inducer, and as such it has been used in numerous AhR studies. However, in contrast to TCDD, 3-MC is not resilient to cellular biotransformation and various 3-MC metabolites have been identified (Wood et al., 1978). The parent compound 3-MC does not bind to the ERs as a *bona fide* ligand (Swedenborg et al., 2008); however, we and others have shown that 3-MC treatment activates ER signaling (Abdelrahim et al., 2006; Swedenborg et al., 2008), most likely via metabolites with estrogenic properties. Similar findings have been reported for other PAHs (Charles et al., 2000; Gozgit et al., 2004; Liu et al., 2006).

In this study, we compared the effects of 3-MC, TCDD and the synthetic estrogen diethylstilbestrol (DES), on estrogen signaling in a HepG2-derived cell line expressing ERα. Gene expression microarrays were used to identify and study gene networks that are controlled by these compounds. Our studies reveal considerable differences between the cellular responses to dioxin and 3-MC at the transcriptional level. Bioinformatic analysis and grouping of the affected genes by function demonstrated that distinct regulatory networks are affected by the different ligands, with surprisingly little overlap between 3-MC and TCDD.

Like DES, 3-MC induced known ER-regulated genes as well as genes that have not been previously reported as ER targets. These findings were confirmed by quantitative PCR in a different cell line. Additionally, recruitment of ERα, but not AhR, was observed to promoter regions of DES and 3-MC induced genes. In contrast to DES, however, the effects of 3-MC were only mediated by ERα but not by ERβ, suggesting an ER subtype-selective mechanism.

2. Materials and methods

2.1. Cell culture and reagents

2,3,7,8-Tetrachlorodibenzo-*p*-dioxin and 3-methylcholanthrene were purchased from AccuStandard (New Haven, CT). 17β-Estradiol and diethylstilbestrol were from Sigma (St. Louis, MO).

HepG2 cells stably transfected with ERα expression vector (Hep-ERα) have been described previously (Barkhem et al., 1997). MCF-7, HepG2 wildtype and Hep-ERα were routinely maintained in Dulbecco's modified Eagle's medium (DMEM; Invitrogen) supplemented with 10% fetal calf serum (FCS; Invitrogen), penicillin (100 U/ml) and streptomycin (100 μg/ml). HepG2 stably transfected with ERE-Luciferase (HepELN), in combination with ERα (HepELN-ERα) or ERβ (HepELN-ERβ), were a kind gift of Patrick Balaguer. HepELN-ERα and HepELN-ERβ were maintained in phenol-red free RPMI (Invitrogen) supplemented with 10% dextran-coated charcoal- (DCC)-treated FCS (HiClone), 1% pen/strep, 1% non-essential amino acids (Invitrogen), 1% sodium pyruvate (Invitrogen) 1 mg/ml G418 (Invitrogen) and 0.5 μg/ml puromycin.

2.2. Microarray analysis

The experimental method used has been described previously (Kanno et al., 2006), with minor modifications. In short, Hep-ERα cells were grown in phenol red-free medium with 5% DCC-treated FCS for 48 h prior the experiment. Treatments for 24 h with vehicle, DES (50 nM), 3-MC (10 μM) or TCDD (10 nM) were carried out in triplicate. For each treatment group, six 10-cm plates were used (two dishes were pooled in order to get at least 2×10^{-6} cells). The cells were rinsed in PBS and harvested in RLT buffer (QIAGEN GmbH, Germany). Total RNA was extracted using RNeasy Mini Kit (QIAGEN) and analyzed by GeneCHIP (Affymetrix).

2.2.1. Bioinformatical analysis

For computer-based analysis, we used the Genomatix software suite, combining BiblioSphere, Gene2Promoter and MatInspector. For gene ontology classification and deciphering signaling networks, BiblioSphere was used. Promoter sequences of selected genes were extracted by Gene2Promoter. For analysis of transcription factor binding sites, we used MatInspector.

2.3. Quantitative real-time PCR

Quantitative real-time PCR was carried out on a subset of genes to validate the regulation observed in the microarray analysis. HepELN control, HepELN-ERα or HepELN-ERβ cells were seeded into 60-cm dishes and grown in phenol red-free medium with 5% DCC-treated FCS for 48 h. After treatment with DES, 3-MC or TCDD for 6 or 20 h, RNA was isolated using Trizol (Invitrogen, CA) according to the manufacturer's recommendations. One microgram of total RNA was treated with DNAseI and reverse transcribed using random hexamer primers (Invitrogen). The resulting cDNA was then used for real-time PCR with Fast SYBR green master mix (Invitrogen) on an ABI 7500 instrument. All gene transcripts were normalized to the 18S rRNA content (internal reference gene) and to the vehicle-treated samples. The analysis was based on the ΔΔCT method.

Primers were designed with the Primer Express software (ABI) and are listed in Table 1.

2.4. Chromatin immunoprecipitation (ChIP) assays

ChIP assays were performed as described (Metivier et al., 2003) with minor modifications. Briefly, HepELN-ERα cells were grown to 80–90% confluency in phenol-red free DMEM supplemented with 5% DCC-stripped FCS for 2 days, before they were treated with vehicle, 50 nM DES, 10 μM 3-MC or 10 nM TCDD for 2 h. Cells were cross-linked with 1.5% formaldehyde for 15 min at room temperature, and washed twice with ice-cold PBS. The cells were collected in 0.5 ml cell collection buffer (100 mM Tris–HCl [pH 9.4] and 10 mM DTT) and incubated on ice for 10 min and subsequently at 30 °C for 15 min. Cells were then lysed sequentially by suspension and 5 min centrifugation at 2000g (4 °C) with 1 ml PBS, 1 ml Nucleus/Chromatin Preparation (NCP) buffer I, (10 mM EDTA, 0.5 mM EGTA, 10 mM HEPES [pH 6.5], 0.25% Triton X-100) and 1 ml NCP II (1 mM EDTA, 0.5 mM EGTA, 10 mM HEPES [pH 6.5], 200 mM NaCl). Finally, chomatin preparations were resuspended in 0.3 ml lysis buffer (10 mM EDTA, 50 mM Tris–HCl [pH 8.1], 1% sodium dodecyl sulfate (SDS), 0.5% Empigen BB), and sonicated in ice water for 10 min with 30 s intervals (Bioruptor, Diagenode Inc.).

After centrifugation, 40 μl of the supernatants were used as inputs, and the remainder diluted 3.5-fold in IP buffer (2 mM EDTA,

Table 1
Top 20 upregulated genes upon 3-MC compared to vehicle treatment.

Accession_No.	Gene_ID	Gene_symbol	Log ratio	Regulation by DES	Regulation by TCDD	ER target gene[a]	ERE	AhR target gene[a]	XRE
NM_000499	1543	CYP1A1	3.821	Down	Up	Matthews et al. (2005)	Predicted	Whitlock (1999)	Whitlock (1999)
NM_000691	218	ALDH3A1	3.104	Down	Up	Sladek (2003)	Not predicted	Vasiliou et al. (1999)	Vasiliou et al. (1999)
NM_000602	5054	SERPINE1	2.523	NR	NR	Burdette and Woodruff (2007)	Predicted	Puga et al. (2000)	Huang and Elferink (2011)
NM_004864	9518	GDF15	2.404	NR	NR		Predicted		Not predicted
NM_018485	27202	GPR77	2.246	Up	NR		Predicted		Not predicted
AK025719	3481	IGF2	2.074	Up	Up	Szabo et al. (2004)	Pathak et al. (2010)		Not predicted
AK095363	360	AQP3	2.07	Down	Up	Moller et al. (2010)	Not predicted		Not predicted
NM_004591	6364	CCL20	1.987	NR	NR		Predicted		Not predicted
NM_014331	23657	SLC7A11	1.986	NR	NR		Not predicted	Burchiel et al. (2007)	Burchiel et al. (2007)
XM_001116862	1026	CDKN1A	1.982	NR	NR	Thomas et al., 1998	Mandal and Davie (2010)	Iseki et al. (2005)	Pang et al. (2008)
XM_517958	1958	EGR1	1.895	NR	NR		Not predicted		Predicted
AK125255	467	ATF3	1.832	NR	Up		Not predicted		Predicted
XM_001136017	3589	IL11	1.767	NR	NR		Predicted		Predicted
NM_001736	728	C5AR1	1.754	NR	Up		Predicted		Not predicted
AK127286	54498	SMOX	1.723	NR	NR		Predicted		Predicted
NM_013409	10468	FST	1.716	Up	NR		Predicted		Predicted
NM_004024	57834	CYP4F11	1.665	NR	NR		Predicted		Not predicted
AK125714	2302	FOXJ1	1.657	NR	NR		Not predicted		Predicted
NM_008240	7102	TSPAN7	1.627	Up	Up		Predicted		Predicted
NM_004615	79083	MLPH	1.611	NR	Up		Predicted		Predicted

NR: not regulated.
[a] ER- and AhR-target genes are defined as genes that are regulated by ER or AhR ligand with a clear involvement of the respective receptor. Prediction of EREs and XREs was made by MatInspector (Genomatix).

150 mM NaCl, 20 mM Tris–HCl [pH 8.1], 1% Triton X-100) with protease inhibitors freshly added (Complete Protease Inhibitor Cocktail tablets; Roche). After 2 h preclearing at 4 °C with 10 μl DCC serum, 2 μg sheared salmon sperm DNA, and 40 μl protein A/G-Sepharose beads (Sigma), the lysates were subjected to overnight immunoprecipitation. Specific antibodies used for precipitation were H184 (ERα), H211 (AhR), H172 (ARNT), all from Santa Cruz Biotechnology, Santa Cruz, CA. Complexes were recovered by a 2 h incubation at 4 °C with 2 μg of sheared salmon sperm DNA and 50 μl of protein A/G-Sepharose. Precipitates were serially washed with 300 μl Washing Buffer (WB) I (2 mM EDTA, 20 mM Tris–HCl [pH 8.1], 0.1% SDS, 1% Triton X-100, 150 mM NaCl), WB II (2 mM EDTA, 20 mM Tris–HCl [pH 8.1], 500 mM NaCl), WB III (1 mM EDTA, 10 mM Tris–HCl [pH 8.01], 1% NP-40, 1% deoxycholate, 0.25 M LiCl) and then three times with 1 mM EDTA, 10 mM Tris–HCl [pH 8.1]. Immunoprecipitated complexes were removed from the beads by extraction with 50 μl of 1% SDS, 0.1 M $NaHCO_3$ for 10 min, vortexing and centrifugation, repeated three times. Cross-linking was reversed by incubation at 65 °C overnight. DNA fragments were isolated and purified with MSB Spin PCRapace (Invitek GmbH, Germany). Real-time PCR was performed as described above with primers listed in Supplementary Table 1.

3. Results

3.1. TCDD and 3-MC regulate distinct gene networks

TCDD and 3-MC are AhR ligands and both affect ER signaling. Although they are frequently used as interchangeable compounds, they have distinct effects on ER transcriptional activity. While TCDD acts solely as ER inhibitor (Safe and Wormke, 2003), at least in the presence of AhR (Abdelrahim et al., 2003), we have shown previously that 3-MC gives rise to metabolites that display estrogenic properties in a cell-type specific fashion (Swedenborg et al., 2008). In order to systematically compare the effects of TCDD and 3-MC on ER signaling, we conducted a whole genome analysis of the transcriptional effects of TCDD and 3-MC, and compared it to the transcriptional response after treatment with diethylstilbestrol (DES), a well-characterized ER ligand.

We analyzed gene expression profiles in HepG2 cells, a human hepatocellular carcinoma cell line, stably expressing ERα at moderate levels (HepG2-ERα, Barkhem et al., 1997). We chose this cell line because it endogenously expresses the AhR signaling machinery and exhibits high metabolic capacity towards 3-MC (Swedenborg et al., 2008) and other substances (Bursztyka et al., 2008). To allow for possible metabolism of 3-MC to occur, a 24 h treatment was chosen. HepG2-ERα cells were treated with vehicle, 50 nM DES, 10 μM 3-MC or 10 nM TCDD, total RNA was prepared and microarray analysis was performed. The analysis included genes that were either induced or repressed by the treatments compared to vehicle-treated cells. The cut-off was set to at least 2-fold change ($p < 0.01$).

Interestingly, comparing the up- and down-regulated genes, there was very little overlap between the three treatments, suggesting that TCDD, 3-MC and DES control separate sets of genes and induce distinct signaling pathways (Fig. 1A). Among those genes whose expression was upregulated by both 3-MC and TCDD, classical AhR target genes like CYP1A1 and aldehyde dehydrogenase 3A1 were identified, which also serve to validate the assay. However, surprisingly few genes were regulated by both 3-MC and TCDD (Fig. 1B), suggesting that these two AhR ligands induce different regulatory networks in the cells, at least after 24 h of treatment.

In cells treated with the ER agonist DES, we identified a wide response including well-characterized estrogen-responsive genes such as GREB1 and TFF1/pS2, confirming that the ER signaling machinery is functional in the cells.

A striking difference between the treatment groups was the high number of genes that were regulated by 3-MC; approximately

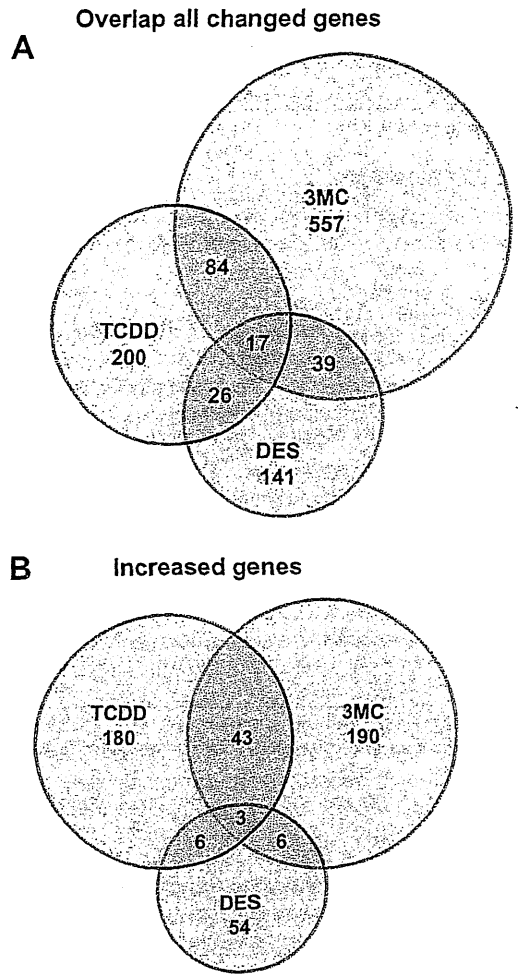

Fig. 1. Microarray data analysis. (A) Venn-diagram depicting the overlap of genes with changed expression upon treatment. (B) Venn-diagram depicting the overlap of genes with increased expression upon treatment.

700 genes with significantly altered expression, twice as many as DES and three times as many as affected by TCDD (see Fig. 1A). This is possibly an effect caused by the multitude of metabolites derived from 3-MC, and their actions within the cell.

In order to assess if the genes induced by 3-MC could be direct AhR or ER targets, we extracted the promoter sequences of the 20 genes whose expression was most up-regulated by 3-MC using the Genomatix software Gene2Promoter. These promoter sequences were analyzed by MatInspector, which retrieves conserved transcription factor binding sites. In the promoter sequences that have no published ERE or XRE sites, the program predicted either ERE or XRE or both sites in all but one (Aquaporin 3) promoter sequences (Table 1). Seven out of the 20 promoters contained one or more predicted or published ERE but no XRE. This was in contrast to the 20 genes whose expression was most up-regulated by TCDD, where only one promoter contained an ERE sequence in the absence of an XRE (data not shown). Thus, this *in silico*-based approach confirmed the presence of putative estrogen receptor binding sites in promoter regions of 3-MC regulated genes, which could suggest that 3-MC or its metabolites induce transcription of these genes by activating estrogen receptor.

The regulated genes were then classified depending on their biological function. Again, this clustering analysis showed that 3-MC and TCDD affected regulatory pathways only partly overlap (Table 2). DES and 3-MC up-regulated mostly genes that are involved in developmental processes. Additionally, genes up-regulated by DES are involved in metabolic processes while 3-MC up-regulated genes act in apoptosis and programmed cell death. In contrast, genes induced by TCDD were found mainly to be involved in nutrient transport and cellular signaling cascades. Developmental processes were only minimally affected by TCDD. Taken together, the results show three distinct chemicals having profoundly different effects in these cells.

3.2. 3-MC activates ER-target genes via ER

To validate the changes in the expression profiles identified by the microarray analysis, a set of regulated genes was chosen and analyzed using quantitative real-time PCR. We chose to use different HepG2-derived cell lines, stably transfected with either ERα (HepELN-ERα) or ERβ (HepELN-ERβ) (Riu et al., 2011). The use of these cell lines allowed us firstly, to show that the findings are not specific for HepG2-ERα cells and secondly, to assess the effects of the treatments on each estrogen receptor subtype separately. Although ERα is the predominant ER isoform in the liver, ERβ has been shown to be expressed and to exert some functions in this tissue (Barros and Gustafsson, 2011), and ERβ signaling is functioning in the HepELN-ERβ cell line (Riu et al., 2011).

HepELN-ERα cells, HepELN-ERβ cells, and the control cell line HepELN lacking ER were treated with DES, 3-MC or TCDD and mRNA levels were determined by quantitative RT-PCR. We chose two exposure times: one similar to the one used for the microarray study (20 h) and a shorter one (6 h). The latter was chosen to test whether the chemicals regulate the investigated genes directly or indirectly by controlling genes upstream of the investigated ones.

For the analysis, we chose the known ER target gene TFF1/pS2, insulin-like growth factor binding protein 4 (IFBP4), also a known ER target gene (Bourdeau et al., 2004; Denger et al., 2008) and the most highly DES-induced gene not induced by 3-MC, plasminogen activator inhibitor-1/Serpine I (PAI-1), which was the most highly 3-MC-induced gene not induced by DES, and follistatin (FST), which was among the top 20 induced by both DES and 3-MC.

As expected, the estrogen DES induced transcription of both known ER-target genes via ERα at both time points (Fig. 2A and B). Induction of transcription via ERβ was less pronounced and only measured after 20 h of treatment. 3-MC induced TFF1/pS2 at both time points, whereas for IGFBP4 induction was only measured at the 6 h time point. Interestingly, 3-MC could induce the two genes only via ERα, whereas no effect via ERβ was observed. TCDD treatment had no effect on the transcription of these two genes.

PAI-1 could be induced by 3-MC at both time points, but again only in ERα-expressing cells (Fig. 2C). The effect of DES was slightly less pronounced and only measurable after 6 h, not after 20 h. The short effect of DES on PAI-1 and of 3-MC on IGFBP4 could explain the discrepancies to the microarray results as the cells were treated for 24 h for the microarray analysis. FST was induced by both compounds, however, only treatment of DES led to increased expression in the ERβ-expressing cells (Fig. 2D).

To conclude, we have identified ER-activated regulation of TFF1/pS2, PAI-1, and FST by the polycyclic aromatic hydrocarbon 3-MC, or by a metabolite of the parent compound. The estrogenic activities exerted by 3-MC, or its derivative, seem to be mediated exclusively by ERα, which suggests an ER isoform-selectivity of the active compound.

3.3. 3-MC induces recruitment of ERα to target gene promoters

Our results so far suggest that 3-MC, or rather a metabolite of this compound, displays estrogenic activities that are dependent

Table 2
Gene ontology (GO) of the genes upregulated by DES, 3-MC, and TCDD.

Term	ID	Total	Observed	Expected	ZScore
Genes up-regulated by DES					
Multicellular organismal process	GO:0032501	2983	23	11.17	3.92
Organ development	GO:0048513	1127	11	4.22	3.43
Cell proliferation	GO:0008283	748	8	2.8	3.19
System development	GO:0048731	1555	13	5.82	3.13
Organ morphogenesis	GO:0009887	369	5	1.38	3.12
Multicellular organismal development	GO:0007275	2113	16	7.91	3.08
Anatomical structure development	GO:0048856	1792	14	6.71	2.99
Carbohydrate metabolic process	GO:0005975	389	5	1.46	2.98
Developmental process	GO:0032502	2925	19	10.95	2.68
Phosphorus metabolic process	GO:0006793	888	8	3.33	2.64
Phosphate metabolic process	GO:0006796	888	8	3.33	2.64
Phosphorylation	GO:0016310	741	7	2.77	2.6
Genes up-regulated by 3-MC					
Regulation of developmental process	GO:0050793	786	18	3.66	7.71
Organ development	GO:0048513	1127	19	5.24	6.24
Developmental process	GO:0032502	2925	34	13.6	6.11
Positive regulation of biological process	GO:0048518	1111	18	5.17	5.86
Regulation of cell differentiation	GO:0045595	176	6	0.82	5.77
Apoptosis	GO:0006915	761	14	3.54	5.71
Negative regulation of transcription from RNA polymerase II promoter	GO:0000122	130	5	0.6	5.69
Programmed cell death	GO:0012501	769	14	3.58	5.66
Epidermis development	GO:0008544	133	5	0.62	5.61
Regulation of phosphorylation	GO:0042325	89	4	0.41	5.6
Cell death	GO:0008219	816	14	3.79	5.39
Death	GO:0016265	816	14	3.79	5.39
Genes up-regulated by TCDD					
Carboxylic acid transport	GO:0046942	79	5	0.38	7.51
Amino acid transport	GO:0006865	56	4	0.27	7.2
Amine transport	GO:0015837	71	4	0.34	6.27
G-protein signaling, coupled to cyclic nucleotide second messenger	GO:0007187	88	4	0.43	5.51
Cyclic-nucleotide-mediated signaling	GO:0019935	95	4	0.46	5.25
Positive regulation of biological process	GO:0048518	1111	16	5.37	4.76
Positive regulation of cellular process	GO:0048522	1008	14	4.87	4.28
Negative regulation of transcription from RNA polymerase II promoter	GO:0000122	130	4	0.63	4.28
Sensory perception of sound	GO:0007605	134	4	0.65	4.19
Anatomical structure development	GO:0048856	1792	20	8.66	4.09
System development	GO:0048731	1555	18	7.51	4.03
Nervous system development	GO:0007399	673	10	3.25	3.83

The GO analysis was carried out using BiblioSphere (Genomatix).

on ERα. To further corroborate a mechanism involving ERα activation, we analyzed ERα recruitment upon 3-MC and DES treatment to IGFBP4, FST, and GREB1 as positive control. To this end, we performed chromatin immunoprecipitations assays (ChIPs) in HepELN-ERα cells. ER recruitment to target promoters is usually seen very shortly after ligand treatment, thus incubation times between 15 and 45 min are normally used in ChIP protocols. We assumed that such a short incubation time would not allow for sufficient accumulation of 3-MC metabolites, thus we treated the cells for 2 h with DES, 3-MC, and TCDD. Precipitations were performed with antibodies against ERα, AhR and ARNT. The precipitated DNA was analyzed by real-time PCR amplifying either known functional EREs (GREB1 promoter (Ruegg et al., 2008), IGFBP4 enhancer (Bourdeau et al., 2004; Denger et al., 2008)) or an ERE in the FST promoter identified by *in silico* analysis (Fig. 3B).

In line with the expression data, the ChIP results show recruitment of ERα to these regions upon treatment with DES or 3-MC, but not with TCDD (Fig. 3A–C). Neither AhR nor ARNT was recruited, suggesting that 3-MC acts via ERα.

In control experiments, a xenobiotic response element (XRE) in the promoter region of the CYP1A1 gene was analyzed in the same cells, and ERα was not found to associate to this region (Fig. 3D). When precipitations were carried out with AhR or ARNT antibodies, we found high enrichment of both AhR and ARNT at the CYP1A1 enhancer in the presence of both 3-MC and TCDD, confirming our treatments and the responsiveness of the cell model.

These findings demonstrate that 3-MC, just like DES, can induce ERα-recruitment to EREs in target genes, independently of ARNT- or AhR-recruitment. This is true not only for known ERα-target genes (like GREB-1 and IGFBP4) but also for FST, identifying FST as a novel ER-target gene.

4. Discussion

TCDD and 3-MC are widely used as prototypical AhR ligands and CYP1A1 inducers, however, their precise biological response patterns have not been characterized. In this study, we compared the transcriptional response to TCDD, 3-MC and DES in HepG2 cells, a cell line that is able to metabolize 3-MC. The microarray analysis showed that, while 24 h treatment with DES and TCDD affected around 200 and 300 genes, respectively, 3-MC treatment significantly altered the expression of almost 700 genes. We suggest that this outcome reflects the high number of metabolites generated by biotransformation of 3-MC in HepG2 cells, and their actions within the cell.

Importantly, 3-MC and TCDD control distinct gene networks and biological functions. 3-MC has frequently been used as an AhR agonist instead of TCDD in both *in vitro* and *in vivo* studies, due to strict national regulations controlling the use of dioxin in laboratories. The findings presented here clearly show that data obtained with 3-MC cannot be generalized for other AhR ligands, particularly not for TCDD.

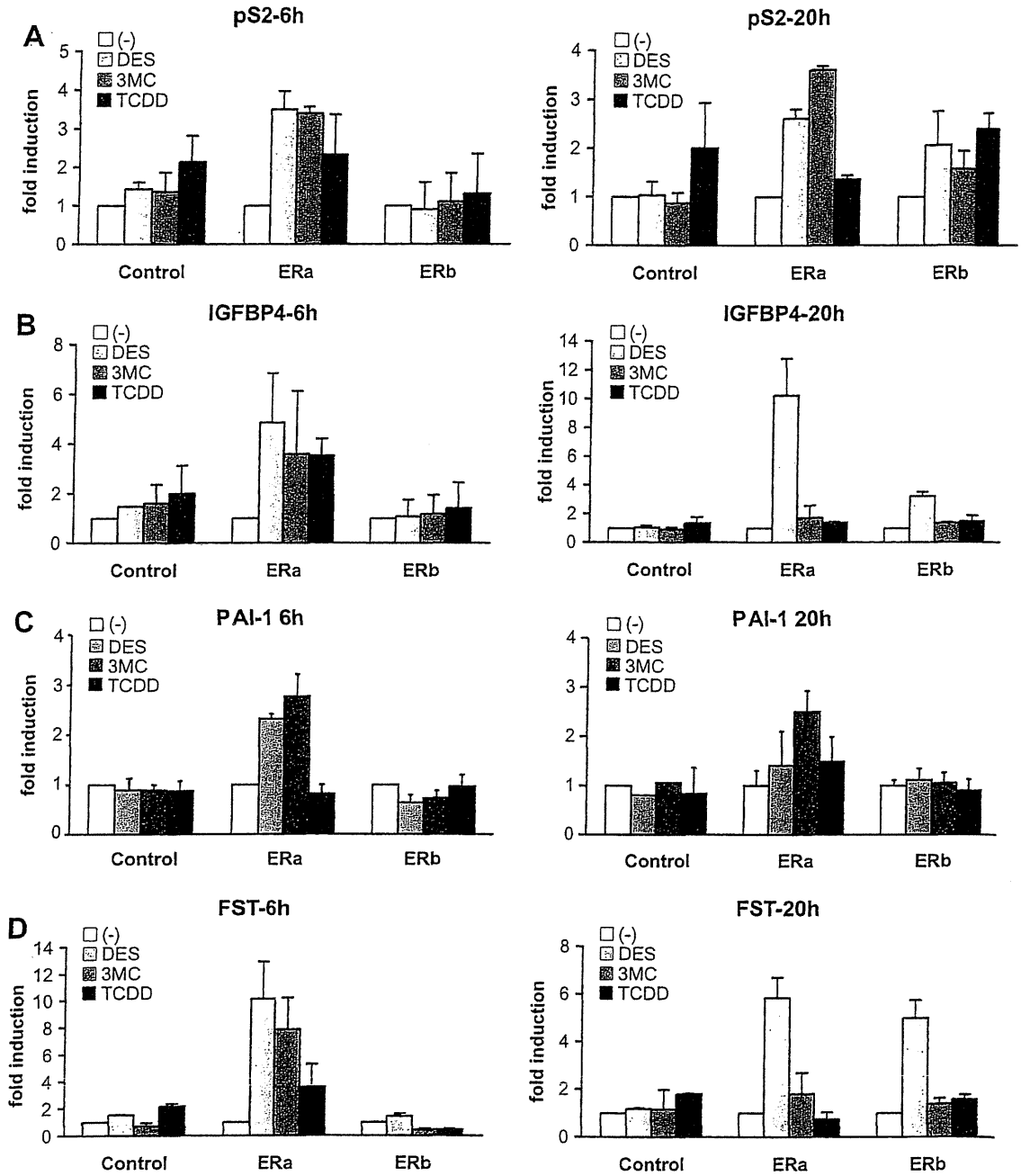

Fig. 2. Validation of microarray data (qRT-PCR). Verification of the microarray data was carried out as described in Materials and methods. Total RNA from control HepELN, HepELN-ERα or HepELN-ERβ cells treated with DES-, 3-MC or TCDD was prepared after 6 h and 20 h. The relative level of mRNA of regulated genes was then analyzed by quantitative RT-PCR. Samples were analyzed in triplicates and are given as SEM. (A) TFF1/pS2; (B) IGFBP-4; (C) PAI-1; (D) FST.

Endocrine disruption has been extensively documented, in particular for the estrogen receptor. TCDD and 3-MC have both been shown to interfere with the ERs but by different mechanisms of action. We and others could demonstrate that 3-MC, or rather some of its metabolites, act as ERα ligands (Abdelrahim et al., 2006; Swedenborg et al., 2008). TCDD, on the other hand, inhibits ER-mediated gene transcription by indirect mechanisms, e.g. by inducing competition between ER and AhR for their common co-activator ARNT (Brunnberg et al., 2003; Ruegg et al., 2008; Safe et al., 2000). In this study, we could confirm that 3-MC can induce ER-target genes in an ERα-dependent manner. The induction was apparent already after 6 h of treatment, suggesting that 3-MC derived compounds act directly on ERα. This notion was corroborated by the finding that ERα is recruited to predicted ERE sequences located in the target gene promoters upon 3-MC treatment. A complex molecular interplay between the AhR and ER can occur on some promoters (Klinge et al., 2000; Matthews et al., 2005; Safe and McDougal, 2002; Safe et al., 2000; Spink et al., 2003; Wang et al., 2001; Wormke et al., 2000; Zacharewski et al., 1994). However, on the promoters analyzed in this study, no co-recruitment of ERα, AhR, and ARNT could be measured.

Intriguingly, the estrogenic effect of 3-MC was only detected in ERα-expressing cells but not in ERβ-expressing cells. This result indicates that, in contrast to DES, the active 3-MC metabolite acts through an isoform-selective mechanism. Again, this is in contrast to TCDD that has been shown to interfere in particular with ERβ (Ruegg et al., 2008).

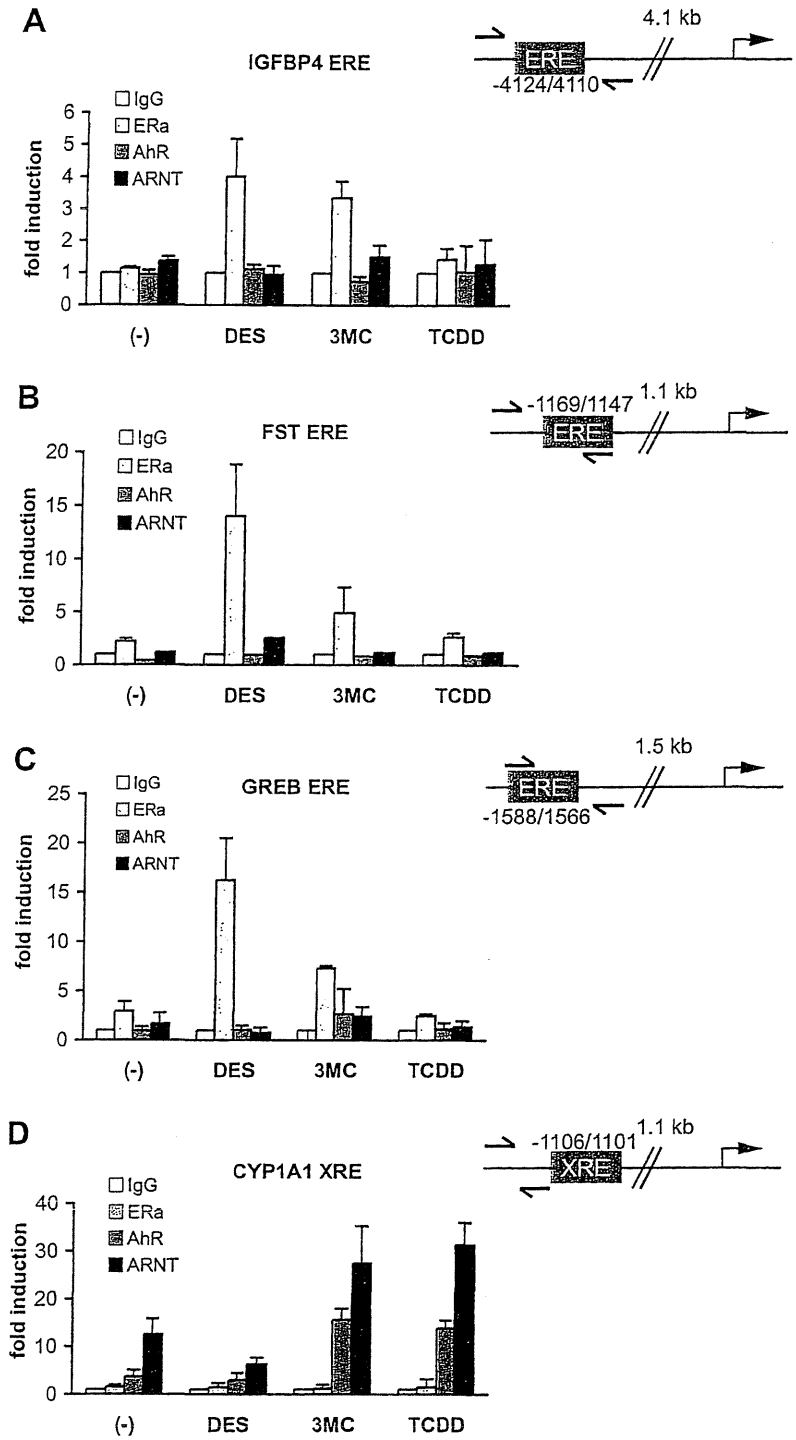

Fig. 3. Chromatin immunoprecipitations (ChIPs). HepELN-ERα cells were treated for 2 h as described in Materials and methods. ChIPs were carried out with antibodies directed against ERα, AhR and ARNT. Enrichment to regulatory regions comprising EREs or an XRE was analyzed with quantitative real-time PCR. (A) IGFBP4 (ERE – 4.1 kb); (B) FST (ERE – 1.1 kb); (C) GREB-1 (ERE – 1.5 kb); (D) CYP1A1 (XRE – 1.1 kb).

In addition to the known ER target genes, DES and 3-MC induced genes that have not been shown previously to be regulated by ER. For FST and PAI-1 we could confirm that they are regulated by activated ERα, FST also by activated ERβ. As their expression was already upregulated after 6 h we speculated that they are novel direct ER target genes. Indeed, we could identify potential ER binding sites in the promoter region of these genes. For FST, we could show DES and 3-MC-dependent ERα-recruitment to a predicted ERE, confirming it to be a direct ERα-target gene. FST is important for the development of bone, muscle, and skin (Matzuk et al., 1995), and is essential for functioning of the female and male gonads (reviewed in e.g. de Kretser et al., 2002). Our finding that 3-MC can induce FST-expression calls for further experiments evaluating the effects of 3-MC on FST in these systems.

5. Conclusions

We have shown that the prototypical AhR ligands TCDD and 3-MC control separate gene regulatory networks and have distinct impacts on the cells. Thus care should be taken when interpreting

studies that use these two compounds interchangeably. In contrast to TCDD, 3-MC induces known estrogen-responsive genes such as GREB1, IGFBP4 and TFF1/pS2 as well as genes not previously reported to be ER target genes, like FST and PAI-1/Serpine1. Furthermore, estrogenicity of 3-MC, or some of its metabolites, is ER isoform-selective, affecting only ERα.

Acknowledgement

We are grateful to Patrick Balaguer, INSERM, Montpellier, France for providing the HepELN cell lines used in this study.

Appendix A. Supplementary data

Supplementary data associated with this article can be found, in the online version, at http://dx.doi.org/10.1016/j.mce.2012.05.006.

References

Abdelrahim, M., Ariazi, E., Kim, K., Khan, S., Barhoumi, R., Burghardt, R., Liu, S., Hill, D., Finnell, R., Wlodarczyk, B., Jordan, V.C., Safe, S., 2006. 3-Methylcholanthrene and other aryl hydrocarbon receptor agonists directly activate estrogen receptor alpha. Cancer Res. 66, 2459–2467.

Abdelrahim, M., Smith 3rd, R., Safe, S., 2003. Aryl hydrocarbon receptor gene silencing with small inhibitory RNA differentially modulates Ah-responsiveness in MCF-7 and HepG2 cancer cells. Mol. Pharmacol. 63, 1373–1381.

Astroff, B., Safe, S., 1990. 2,3,7,8-Tetrachlorodibenzo-p-dioxin as an antiestrogen: effect on rat uterine peroxidase activity. Biochem. Pharmacol. 39, 485–488.

Barkhem, T., Andersson-Ross, C., Hoglund, M., Nilsson, S., 1997. Characterization of the "estrogenicity" of tamoxifen and raloxifene in HepG2 cells: regulation of gene expression from an ERE controlled reporter vector versus regulation of the endogenous SHBG and PS2 genes. J. Steroid Biochem. Mol. Biol. 62, 53–64.

Barros, R.P., Gustafsson, J.A., 2011. Estrogen receptors and the metabolic network. Cell Metab. 14, 289–299.

Bourdeau, V., Deschenes, J., Metivier, R., Nagai, Y., Nguyen, D., Bretschneider, N., Gannon, F., White, J.H., Mader, S., 2004. Genome-wide identification of high-affinity estrogen response elements in human and mouse. Mol. Endocrinol. 18, 1411–1427.

Boverhof, D.R., Burgoon, L.D., Williams, K.J., Zacharewski, T.R., 2008. Inhibition of estrogen-mediated uterine gene expression responses by dioxin. Mol. Pharmacol. 73, 82–93.

Brunnberg, S., Pettersson, K., Rydin, E., Matthews, J., Hanberg, A., Pongratz, I., 2003. The basic helix-loop-helix-PAS protein ARNT functions as a potent coactivator of estrogen receptor-dependent transcription. Proc. Natl. Acad Sci. USA 100, 6517–6522.

Burchiel, S.W., Thompson, T.A., Lauer, F.T., Oprea, T.I., 2007. Activation of dioxin response element (DRE)-associated genes by benzo(a)pyrene 3,6-quinone and benzo(a)pyrene 1,6-quinone in MCF-10A human mammary epithelial cells. Toxicol. Appl. Pharmacol. 221, 203–214.

Burdette, J.E., Woodruff, T.K., 2007. Activin and estrogen crosstalk regulates transcription in human breast cancer cells. Endocr. Relat. Cancer 14, 679–689.

Bursztyka, J., Perdu, E., Pettersson, K., Pongratz, I., Fernandez-Cabrera, M., Olea, N., Debrauwer, L., Zalko, D., Cravedi, J.P., 2008. Biotransformation of genistein and bisphenol A in cell lines used for screening endocrine disruptors. Toxicol. In Vitro 22, 1595–1604.

Chaloupka, K., Krishnan, V., Safe, S., 1992. Polynuclear aromatic hydrocarbon carcinogens as antiestrogens in MCF-7 human breast cancer cells: role of the Ah receptor. Carcinogenesis 13, 2233–2239.

Charles, G.D., Bartels, M.J., Zacharewski, T.R., Gollapudi, B.B., Freshour, N.L., Carney, E.W., 2000. Activity of benzo[a]pyrene and its hydroxylated metabolites in an estrogen receptor-alpha reporter gene assay. Toxicol. Sci. 55, 320–326.

de Kretser, D.M., Hedger, M.P., Loveland, K.L., Phillips, D.J., 2002. Inhibins, activins and follistatin in reproduction. Hum. Reprod. Update 8, 529–541.

Denger, S., Bahr-Ivacevic, T., Brand, H., Reid, G., Blake, J., Seifert, M., Lin, C.Y., May, K., Benes, V., Liu, E.T., Gannon, F., 2008. Transcriptome profiling of estrogen-regulated genes in human primary osteoblasts reveals an osteoblast-specific regulation of the insulin-like growth factor binding protein 4 gene. Mol. Endocrinol. 22, 361–379.

Elobeid, M.A., Allison, D.B., 2008. Putative environmental-endocrine disruptors and obesity: a review. Curr. Opin. Endocrinol. Diabetes Obes. 15, 403–408.

Gozgit, J.M., Nestor, K.M., Fasco, M.J., Pentecost, B.T., Arcaro, K.F., 2004. Differential action of polycyclic aromatic hydrocarbons on endogenous estrogen-responsive genes and on a transfected estrogen-responsive reporter in MCF-7 cells. Toxicol. Appl. Pharmacol. 196, 58–67.

Harper, N., Wang, X., Liu, H., Safe, S., 1994. Inhibition of estrogen-induced progesterone receptor in MCF-7 human breast cancer cells by aryl hydrocarbon (Ah) receptor agonists. Mol. Cell Endocrinol. 104, 47–55.

Huang, G., Elferink, C.J., 2011. A novel non-consensus xenobiotic response element capable of mediating aryl hydrocarbon receptor dependent gene expression. Mol. Pharmacol.

Iseki, M., Ikuta, T., Kobayashi, T., Kawajiri, K., 2005. Growth suppression of Leydig TM3 cells mediated by aryl hydrocarbon receptor. Biochem. Biophys. Res. Commun. 331, 902–908.

Kanno, J., Aisaki, K., Igarashi, K., Nakatsu, N., Ono, A., Kodama, Y., Nagao, T., 2006. "Per cell" normalization method for mRNA measurement by quantitative PCR and microarrays. BMC Genom. 7, 64.

Kharat, I., Saatcioglu, F., 1996. Antiestrogenic effects of 2,3,7,8-tetrachlorodibenzo-p-dioxin are mediated by direct transcriptional interference with the liganded estrogen receptor. Cross-talk between aryl hydrocarbon- and estrogen-mediated signaling. J. Biol. Chem. 271, 10533–10537.

Klinge, C.M., Kaur, K., Swanson, H.I., 2000. The aryl hydrocarbon receptor interacts with estrogen receptor alpha and orphan receptors COUP-TFI and ERRalpha1. Arch. Biochem. Biophys. 373, 163–174.

Liu, S., Abdelrahim, M., Khan, S., Ariazi, E., Jordan, V.C., Safe, S., 2006. Aryl hydrocarbon receptor agonists directly activate estrogen receptor alpha in MCF-7 breast cancer cells. Biol. Chem. 387, 1209–1213.

Mandal, S., Davie, J.R., 2010. Estrogen regulated expression of the p21 Waf1/Cip1 gene in estrogen receptor positive human breast cancer cells. J. Cell Physiol. 224, 28–32.

Matthews, J., Wihlen, B., Thomsen, J., Gustafsson, J.A., 2005. Aryl hydrocarbon receptor-mediated transcription: ligand-dependent recruitment of estrogen receptor alpha to 2,3,7,8-tetrachlorodibenzo-p-dioxin-responsive promoters. Mol. Cell Biol. 25, 5317–5328.

Matzuk, M.M., Lu, N., Vogel, H., Sellheyer, K., Roop, D.R., Bradley, A., 1995. Multiple defects and perinatal death in mice deficient in follistatin. Nature 374, 360–363.

Metivier, R., Penot, G., Hubner, M.R., Reid, G., Brand, H., Kos, M., Gannon, F., 2003. Estrogen receptor-alpha directs ordered, cyclical, and combinatorial recruitment of cofactors on a natural target promoter. Cell 115, 751–763.

Moller, F.J., Diel, P., Zierau, O., Hertrampf, T., Maass, J., Vollmer, G., 2010. Long-term dietary isoflavone exposure enhances estrogen sensitivity of rat uterine responsiveness mediated through estrogen receptor alpha. Toxicol. Lett. 196, 142–153.

Mukherjee, S., Koner, B.C., Ray, S., Ray, A., 2006. Environmental contaminants in pathogenesis of breast cancer. Indian J. Exp. Biol. 44, 597–617.

Newbold, R.R., Padilla-Banks, E., Jefferson, W.N., Heindel, J.J., 2008. Effects of endocrine disruptors on obesity. Int. J. Androl. 31, 201–208.

Nilsson, S., Makela, S., Treuter, E., Tujague, M., Thomsen, J., Andersson, G., Enmark, E., Pettersson, K., Warner, M., Gustafsson, J.A., 2001. Mechanisms of estrogen action. Physiol. Rev. 81, 1535–1565.

Nomura, T., 2008. Transgenerational effects from exposure to environmental toxic substances. Mutat. Res. 659, 185–193.

Pang, P.H., Lin, Y.H., Lee, Y.H., Hou, H.H., Hsu, S.P., Juan, S.H., 2008. Molecular mechanisms of p21 and p27 induction by 3-methylcholanthrene, an aryl-hydrocarbon receptor agonist, involved in antiproliferation of human umbilical vascular endothelial cells. J. Cell Physiol. 215, 161–171.

Pathak, S., D'Souza, R., Ankolkar, M., Gaonkar, R., Balasinor, N.H., 2010. Potential role of estrogen in regulation of the insulin-like growth factor2-H19 locus in the rat testis. Mol. Cell Endocrinol. 314, 110–117.

Poland, A., Knutson, J.C., 1982. 2,3,7,8-Tetrachlorodibenzo-p-dioxin and related halogenated aromatic hydrocarbons: examination of the mechanism of toxicity. Annu. Rev. Pharmacol. Toxicol. 22, 517–554.

Puga, A., Barnes, S.J., Chang, C., Zhu, H., Nephew, K.P., Khan, S.A., Shertzer, H.G., 2000. Activation of transcription factors activator protein-1 and nuclear factor-kappaB by 2,3,7,8-tetrachlorodibenzo-p-dioxin. Biochem. Pharmacol. 59, 997–1005.

Riu, A., Grimaldi, M., le Maire, A., Bey, G., Phillips, K., Boulahtouf, A., Perdu, E., Zalko, D., Bourguet, W., Balaguer, P., 2011. Peroxisome proliferator-activated receptor gamma is a target for halogenated analogs of bisphenol A. Environ. Health Perspect. 119, 1227–1232.

Ruegg, J., Penttinen-Damdimopoulou, P., Makela, S., Pongratz, I., Gustafsson, J.A., 2009. Receptors mediating toxicity and their involvement in endocrine disruption. EXS 99, 289–323.

Ruegg, J., Swedenborg, E., Wahlstrom, D., Escande, A., Balaguer, P., Pettersson, K., Pongratz, I., 2008. The transcription factor aryl hydrocarbon receptor nuclear translocator functions as an estrogen receptor beta-selective coactivator, and its recruitment to alternative pathways mediates antiestrogenic effects of dioxin. Mol. Endocrinol. 22, 304–316.

Safe, S., McDougal, A., 2002. Mechanism of action and development of selective aryl hydrocarbon receptor modulators for treatment of hormone-dependent cancers (review). Int. J. Oncol. 20, 1123–1128.

Safe, S., Wormke, M., 2003. Inhibitory aryl hydrocarbon receptor–estrogen receptor alpha cross-talk and mechanisms of action. Chem. Res. Toxicol. 16, 807–816.

Safe, S., Wormke, M., Samudio, I., 2000. Mechanisms of inhibitory aryl hydrocarbon receptor-estrogen receptor crosstalk in human breast cancer cells. J. Mammary Gland Biol. Neoplasia 5, 295–306.

Sladek, N.E., 2003. Transient induction of increased aldehyde dehydrogenase 3A1 levels in cultured human breast (adeno)carcinoma cell lines via 5′-upstream xenobiotic, and electrophile, responsive elements is, respectively, estrogen receptor-dependent and -independent. Chem. Biol. Interact. 143–144, 63–74.

Spink, D.C., Katz, B.H., Hussain, M.M., Pentecost, B.T., Cao, Z., Spink, B.C., 2003. Estrogen regulates Ah responsiveness in MCF-7 breast cancer cells. Carcinogenesis 24, 1941–1950.

Swedenborg, E., Ruegg, J., Hillenweck, A., Rehnmark, S., Faulds, M.H., Zalko, D., Pongratz, I., Pettersson, K., 2008. 3-Methylcholanthrene displays dual effects on estrogen receptor (ER) alpha and ER beta signaling in a cell-type specific fashion. Mol. Pharmacol. 73, 575–586.

Swedenborg, E., Ruegg, J., Makela, S., Pongratz, I., 2009. Endocrine disruptive chemicals: mechanisms of action and involvement in metabolic disorders. J. Mol. Endocrinol.

Szabo, P.E., Pfeifer, G.P., Mann, J.R., 2004. Parent-of-origin-specific binding of nuclear hormone receptor complexes in the H19-Igf2 imprinting control region, Mol. Cell Biol. 24, 4858–4868.

Thomas, T.J., Faaland, C.A., Adhikarakunnathu, S., Watkins, L.F., Thomas, T., 1998. Induction of p21 (CIP1/WAF1/SID1) by estradiol in a breast epithelial cell line transfected with the recombinant estrogen receptor gene: a possible mechanism for a negative regulatory role of estradiol. Breast Cancer Res. Treat. 47, 181–193.

Vasiliou, V., Reuter, S.F., Williams, S., Puga, A., Nebert, D.W., 1999. Mouse cytosolic class 3 aldehyde dehydrogenase (Aldh3a1): gene structure and regulation of constitutive and dioxin-inducible expression. Pharmacogenetics 9, 569–580.

Vidaeff, A.C., Sever, L.E., 2005. In utero exposure to environmental estrogens and male reproductive health: a systematic review of biological and epidemiologic evidence. Reprod. Toxicol. 20, 5–20.

Wang, F., Samudio, I., Safe, S., 2001. Transcriptional activation of cathepsin D gene expression by 17beta-estradiol: mechanism of aryl hydrocarbon receptor-mediated inhibition. Mol. Cell Endocrinol. 172, 91–103.

Whitlock Jr., J.P., 1999. Induction of cytochrome P4501A1. Annu. Rev. Pharmacol. Toxicol. 39, 103–125.

Wood, A.W., Chang, R.L., Levin, W., Thomas, P.E., Ryan, D., Stoming, T.A., Thakker, D.R., Jerina, D.M., Conney, A.H., 1978. Metabolic activation of 3-methylcholanthrene and its metabolites to products mutagenic to bacterial and mammalian cells. Cancer Res. 38, 3398–3404.

Wormke, M., Castro-Rivera, E., Chen, I., Safe, S., 2000. Estrogen and aryl hydrocarbon receptor expression and crosstalk in human Ishikawa endometrial cancer cells. J. Steroid Biochem. Mol. Biol. 72, 197–207.

Zacharewski, T.R., Bondy, K.L., McDonell, P., Wu, Z.F., 1994. Antiestrogenic effect of 2,3,7,8-tetrachlorodibenzo-p-dioxin on 17 beta-estradiol-induced pS2 expression. Cancer Res. 54, 2707–2713.

Reproductive Toxicology 34 (2012) 93–100

Contents lists available at SciVerse ScienceDirect

Reproductive Toxicology

journal homepage: www.elsevier.com/locate/reprotox

Increased cellular distribution of vimentin and Ret in the cingulum induced by developmental hypothyroidism in rat offspring maternally exposed to anti-thyroid agents

Hitoshi Fujimoto[a], Gye-Hyeong Woo[a], Kaoru Inoue[a], Katsuhide Igarashi[b], Jun Kanno[b], Masao Hirose[c], Akiyoshi Nishikawa[d], Makoto Shibutani[a,e,*]

[a] Division of Pathology, National Institute of Health Sciences, 1–18–1 Kamiyoga, Setagaya-ku, Tokyo 158-8501, Japan
[b] Division of Molecular Toxicology, National Institute of Health Sciences, 1–18–1 Kamiyoga, Setagaya-ku, Tokyo 158-8501, Japan
[d] Biological Safety Research Center, National Institute of Health Sciences, 1–18–1 Kamiyoga, Setagaya-ku, Tokyo 158-8501, Japan
[c] Food Safety Commission, 5–2–20 Akasaka Park Bld. 22nd Floor, Akasaka, Minato-ku, Tokyo 107-6122, Japan
[e] Laboratory of Veterinary Pathology, Tokyo University of Agriculture and Technology, 3–5–8 Saiwai-cho, Fuchu-shi, Tokyo 183-8509, Japan

ARTICLE INFO

Article history:
Received 4 December 2011
Received in revised form 19 February 2012
Accepted 16 March 2012
Available online 6 April 2012

Keywords:
Developmental hypothyroidism
Cerebral white matter
Vimentin
Ret
Rat

ABSTRACT

To elucidate target molecules of white matter development responding to hypothyroidism, global gene expression profiling of cerebral white matter from male rat offspring was performed after maternal exposure to anti-thyroid agents, 6-propyl-2-thiouracil and methimazole, on postnatal day 20. Genes involved in central nervous system development commonly up- or down-regulated among groups treated with anti-thyroid agents. Immunohistochemical distributions of vimentin, Ret proto-oncogene (Ret), deleted in colorectal cancer protein (DCC), and Claudin11 (Cld11) were examined based on the gene expression profile. Immunoreactive cells for vimentin and Ret in the cingulum, and the immunoreactive intensity of Cld11 and DCC in whole white matter were increased by treatment with anti-thyroid agents. Immunoreactive cells for vimentin and Ret were immature astrocytes and oligodendrocytes, respectively. Thus, immunoreactive cells for vimentin and Ret may be quantitatively measurable targets of developmental hypothyroidism in white matter.

1. Introduction

Thyroid hormones are essential for normal fetal and neonatal brain development, control neuronal and glial proliferation in definitive brain regions and regulate neuronal migration and differentiation [1–3]. In humans, maternal hypothyroxinemia early in pregnancy may adversely affect fetal brain development, and importantly, even mild to moderate hypothyroxinemia may result in suboptimal neurodevelopment [4], thereby increasing the concern of impaired brain development induced by exposure to thyroid hormone-disrupting chemicals in the environment.

Developmental hypothyroidism leads to growth retardation, neurological defects and impaired performance in various behavioral learning actions [5,6]. Rat offspring maternally exposed to anti-thyroid agents, such as 6-propyl-2-thiouracil (PTU) and methimazole (MMI), show impaired brain growth including white matter hypoplasia with decreased axonal myelination and oligodendrocytes, and impairment of neurogenesis, neuronal migration, dendritic arborization and synapse formation [2,7–9]. These types of impaired brain growth are permanent and accompanied by apparent structural and functional abnormalities. However, the molecular mechanism of impaired brain growth is still unclear.

Histological lesion-specific gene expression profiling provides valuable information on the mechanisms underlying lesion development. In previous studies, we established molecular analysis methods for DNA, RNA and proteins in paraffin-embedded small tissue specimens using the organic solvent-based fixative methacarn, with high performance similar to that of unfixed frozen tissue specimens [10–12]. These methods have been used to analyze global gene expression changes in microdissected lesions [13–15].

Abbreviations: CC, corpus callosum; Cld11, claudin 11; CNS, central nervous system; DCC, deleted in colorectal cancer protein; GAPDH, glyceraldehyde 3-phosphate dehydrogenase; GD, gestation day; GDNF, glial cell line-derived neurotrophic factor; GFAP, glial fibrillary acidic protein; MMI, methimazole; OSP, oligodendrocyte specific protein; PCR, polymerase chain reaction; PND, postnatal day; PTU, 6-propyl-2-thiouracil; Ret, Ret proto-oncogene; RT, reverse transcription; v-Maf, v-maf musculoaponeurotic fibrosarcoma oncogene; Zfhx1b, zinc finger homeobox 1b.

* Corresponding author at: Laboratory of Veterinary Pathology, Tokyo University of Agriculture and Technology, 3–5–8 Saiwai-cho, Fuchu-shi, Tokyo 183-8509, Japan. Tel.: +81 42 367 5874; fax: +81 42 367 5771.
E-mail address: mshibuta@cc.tuat.ac.jp (M. Shibutani).

0890-6238/$ – see front matter © 2012 Elsevier Inc. All rights reserved.
http://dx.doi.org/10.1016/j.reprotox.2012.03.005

To evaluate in vivo developmental brain growth effects of thyroid hormone-disrupting chemicals, we morphometrically analyzed neuronal migration and white matter development in a rat developmental hypothyroidism model [16]. Molecules involved in aberrant neurogenesis and neuronal mismigration were identified by global gene expression analysis of the hippocampal area [15]. In the present study, to elucidate marker molecules in white matter involved in developmental hypothyroidism, we performed global gene expression profiling using microarrays. To obtain the white matter-specific gene expression profile, a microdissection technique was applied to the corpus callosum (CC) and bilateral cerebral white matter. Based on expression profiles, cellular localization of selected molecules was then immunohistochemically examined in cerebral white matter after developmental exposure to anti-thyroid agents.

2. Materials and methods

2.1. Chemicals and animals

6-propyl-2-thiouracil (PTU; CAS No. 51-52-9) and methimazole (MMI; CAS No. 60-56-0) were purchased from Sigma Chemical Co. (St. Louis, MO). Pregnant CD® (SD) IGS rats at gestational day (GD) 3 (GD 0: the day vaginal plugs appeared) were purchased from Charles River Japan Inc. (Yokohama, Japan). Animals were individually housed in polycarbonate cages (SK-Clean, 41.5 cm × 26 cm × 17.5 cm; CLEA Japan Inc., Tokyo, Japan) with wood chip bedding (Sankyo Lab Service Corp., Tokyo, Japan) and maintained in a climate-controlled animal room (24 ± 1 °C, relative humidity: 55 ± 5%) with a 12 h light/dark cycle. A soy-free diet (Oriental Yeast Co. Ltd., Tokyo, Japan) was chosen as the basal diet for maternal animals to eliminate possible phytoestrogen effects [17]. Animals received food and water ad libitum throughout experimentation including a 1 week acclimation period.

2.2. Experimental design

Animal experiments are described elsewhere [16]. Briefly, maternal animals were randomly divided into four groups including an untreated control. Eight dams per group were treated with 3 or 12 ppm PTU or 200 ppm MMI, which was added to drinking water from GD 10 to postnatal day (PND) 20 (PND 0: the day of delivery). On PND 2, four male and four female offspring per dam were randomly selected and remaining litters were culled. On PND 20, 20 male and 20 female offspring (at least one male and one female per dam) per group were subjected to prepubertal necropsy [16,18]. All animals were weighed and sacrificed by exsanguination from the abdominal aorta under deep anesthesia with ether. Animal protocols were reviewed and approved by the Animal Care and Use Committee of the National Institute of Health Sciences, Japan.

2.3. Preparation of tissue specimens and microdissection

For microarray and real-time reverse transcription (RT)-polymerase chain reaction (PCR) analyses, the whole brain of male offspring was immediately removed at prepubertal necropsy on PND 20 (n = 4/group) and fixed with methacarn solution for 2 h at 4 °C [10]. Coronal brain slices taken at −3.5 mm from the bregma were dehydrated and embedded in paraffin. Embedded tissues were stored at 4 °C until tissue sectioning for microdissection [19].

For microdissection, 4 and 20 μm-thick serial sections were prepared. The 4 μm-thick sections were stained with hematoxylin and eosin for confirmation of anatomical orientation of the hippocampal substructure to aid microdissection (Fig. 1). The 20 μm-thick sections were mounted onto PEN-foil film (Leica Microsystems GmbH, Welzlar, Germany) overlaid on glass slides, dried in an incubator overnight at 37 °C, and then stained using an LCM staining kit (Ambion, Inc., Austin, TX). Regions of CC and bilateral cerebral white matter (external capsule) in sections, as shown in Fig. 1, were subjected to laser microbeam microdissection (Leica Microsystems GmbH). Forty sections from each animal were used for microdissection, and microdissected samples were individually stored in 1.5 ml tubes at −80 °C until total RNA extraction.

2.4. RNA preparation, amplification and microarray analysis

Total RNA extraction from microdissected regions, quantitation of RNA yield, and RNA amplification were performed using methods described elsewhere [14,15,19].

For microarray analysis, second-round-amplified biotin-labeled antisense RNAs were subjected to hybridization with a GeneChip® Rat Genome 230 2.0 Array (Affymetrix, Inc., Santa Clara, CA).

Gene selection and normalization of expression data were performed using GeneSpring® software 7.2 (Silicon Genetics, Redwood City, CA). Per chip normalization was performed according to a method described elsewhere [14,15]. Genes with expression changes of at least 2-fold in magnitude compared with those of untreated controls were selected. Common genes with altered expression in anti-thyroid agent exposed groups were also selected.

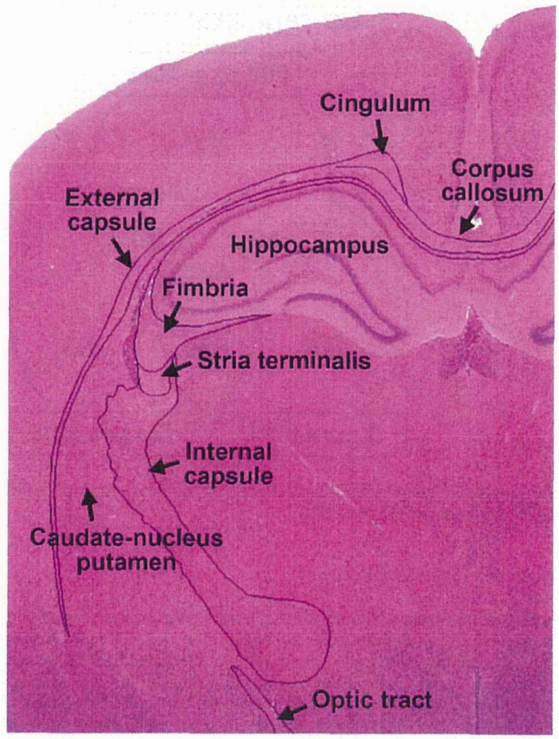

Fig. 1. Overview of the cerebral hemisphere of a male rat at PND 20 stained with hematoxylin and eosin. Magnification, 12.5×.

2.5. Real-time RT-PCR

Quantitative real-time RT-PCR using an ABI Prism 7900HT (Applied Biosystems Japan Ltd., Tokyo, Japan) was performed for confirmation of expression values obtained from microarray analysis. Selected genes showed altered expression (≥2-fold, ≤0.5-fold) in any of the anti-thyroid agent-exposed animals as compared with those of untreated controls. For example, vimentin, *Ret*, v-maf musculoaponeurotic fibrosarcoma oncogene (*v-Maf*) and tektin 4 as up-regulated genes, and *Cld11* and zinc finger homeobox 1b (*Zfhx1b*) as down-regulated ones. RT was performed using first-round antisense RNAs prepared for microarray analysis. For real-time PCR analysis, ABI Assays-on-Demand™ TaqMan® probe and primer sets from Applied Biosystems (n = 4/group) were used. For quantification of expression data, a standard curve method was applied. Expression values were normalized to glyceraldehyde 3-phosphate dehydrogenase (GAPDH) using TaqMan® Rodent GAPDH Control Reagents (Applied Biosystems Japan Ltd.).

2.6. Immunohistochemistry

To evaluate the immunohistochemical distribution of molecules identified by microarray analysis, the brains of male pups obtained at PND 20 were fixed in Bouin's solution at room temperature overnight. Ten animals for each group were used except for the untreated control group with six animals.

Antibodies against vimentin (mouse monoclonal antibody, 1:200; Millipore Corporation, Billerica, MA), glial fibrillary acidic protein (GFAP, rabbit polyclonal antibody, 1:500; Dako, Glostrup, Denmark), Ret (rabbit polyclonal antibody, 1:50; Santa Cruz Biotechnology, Inc., Santa Cruz, CA), DCC (mouse monoclonal antibody, 1:40; Leica Microsystems GmbH), and oligodendrocyte specific protein (OSP, same as Cld11, rabbit polyclonal antibody, 1:200; Novus Biologicals, Inc., Co., Littleton, CO) were used for immunohistochemistry. For antigen retrieval, sections were heated in 10 mM citrate buffer in a microwave for 10 min before incubation with anti-vimentin and -DCC antibodies. Immunodetection was carried out using a VECTASTAIN® Elite ABC kit (Vector Laboratories Inc., Burlingame, CA) with 3,3′-diaminobenzidine/H_2O_2 for the chromogen as described elsewhere [13,14]. Sections were then counterstained with hematoxylin and coverslipped for microscopic examination.

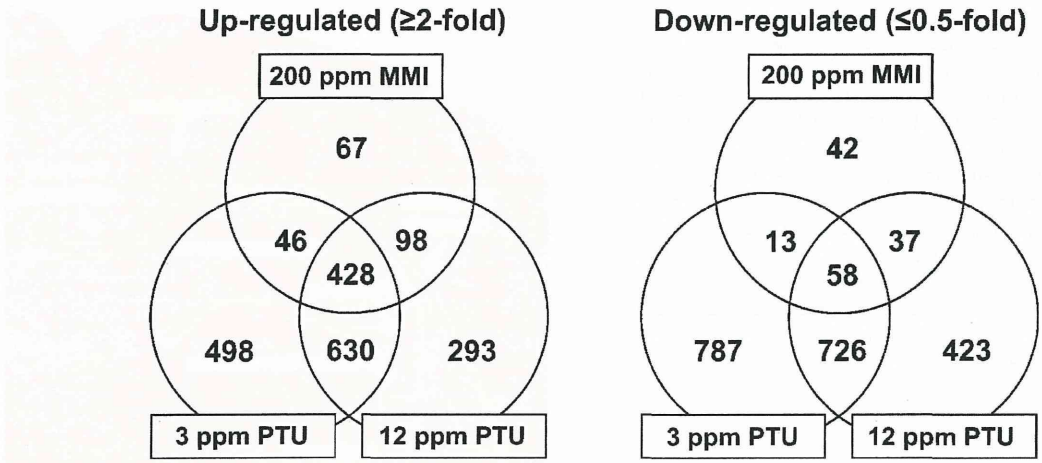

Fig. 2. Venn diagram of genes with altered expression in microarray analysis in response to maternal exposure to anti-thyroid agents. (Left) Up-regulated genes (≥2-fold). (Right) Down-regulated genes (≤0.5-fold).

2.7. Morphometry of immunolocalized cells

The number of immunoreactive cells was quantitatively measured by vimentin and Ret expression in white matter at the cingulum of the bilateral sides using two sections with an approximately 100 μm interval (i.e. four images per animal; Fig. 1), and values were normalized and expressed as those in the unit area (cm^2). GFAP-immunoreactive cells were similarly measured. For quantitative measurement of each immunoreactive cellular component containing vimentin, Ret and GFAP, digital photomicrographs at 100-fold magnification were taken using a BX51 microscope (Olympus Optical Co., Ltd., Tokyo, Japan) attached to a DP70 Digital Camera System (Olympus Optical Co.), and quantitative measurements were performed using WinROOF image analysis software 5.7 (Mitani Corp., Fukui, Japan). To evaluate immunoreactivity of DCC and Cld11 in white matter, staining intensity was scored as 0 (none), 1 (minimal), 2 (slight), 3 (moderate) and 4 (strong) by observation at 40-fold magnification.

2.8. Statistical analysis

Numerical data were assessed by one-way analysis of variance or the Kruskal–Wallis test following Bartlett's test. Statistically significant differences were analyzed by Dunnett's multiple test for comparison with that of the untreated control group. For grading immunohistochemical findings, scores of DCC and Cld11 expression were analyzed with the Mann-Whitney's *U*-test between the untreated control group and each anti-thyroid agent treated group.

3. Results

3.1. Global gene expression analysis

Fig. 2 shows the Venn diagram of genes with altered expression in microdissected cerebral white matter in treated groups in combination or individually in each treated group. Numerous common genes were found to be up- or down-regulated in two of the three treatment groups. The number of genes with up- or down-regulation in response to 3 ppm PTU was higher compared with that of 12 ppm PTU. The number of genes with

Table 1
List of representative genes associated with brain development showing up- or down-regulation common to treatments with MMI and PTU at both 3 and 12 ppm (≥2-fold, ≤0.5-fold).

Accession no.	Gene title	Symbol	MMI	PTU, 3 ppm	PTU, 12 ppm
Up-regulated (20 genes)					
NM_052803	ATPase, Cu++ transporting, alpha polypeptide	*Atp7a*	5.02	11.39	11.09
NM_001108322	T-box 1	*Tbx1*	4.20	4.34	2.31
NM_001191609	Laminin, alpha 5	*Lama5*	4.11	11.57	9.35
NM_031550	Cyclin-dependent kinase inhibitor 2A	*Cdkn2a*	3.59	2.70	3.37
NM_001114330	Glutamate receptor, metabotropic 1	*Grm1*	3.45	2.92	5.89
(NM_001114330)			(3.01)	(2.85)	(2.88)
NM_023091	gamma-Aminobutyric acid A receptor, epsilon	*Gabre*	3.20	3.91	7.46
NM_001107692	Ephrin A4	*Efna4*	3.13	5.07	6.72
NM_001002805	Complement component 4a	*C4a*	3.04	7.15	6.43
NM_019328	Nuclear receptor subfamily 4, group A, member 2	*Nr4a2*	2.97	2.87	4.92
NM_001110099	Ret proto-oncogene	*Ret*	2.89	5.01	4.39
NM_053629	Follistatin-like 3	*Fstl3*	2.85	4.28	6.08
NM_053708	Gastrulation brain homeobox 2	*Gbx2*	2.82	4.73	4.09
NM_019236	Hairy and enhancer of split 2	*Hes2*	2.76	2.93	3.11
NM_001109223	Wingless-related MMTV integration site 16	*Wnt16*	2.71	2.42	3.82
XM_001077495	Nuclear receptor co-repressor 1	*Ncor1*	2.67	2.01	2.97
NM_001012220	Cation channel, sperm associated 2	*Catsper2*	2.54	6.69	4.56
NM_001024275	Ras association (RalGDS/AF-6) domain family 4	*Rassf4*	2.31	4.67	5.43
NM_138900	Complement component 1, s subcomponent	*C1s*	2.12	3.31	3.88
NM_031140	Vimentin	*Vim*	2.11	6.01	4.27
NM_053555	Vesicle-associated membrane protein 5	*Vamp5*	2.04	2.62	3.41
Down-regulated (4 genes)					
NM_013107	Bone morphogenetic protein 6	*Bmp6*	0.23	0.38	0.25
NM_053759	Sine oculis homeobox homolog 1	*Six1*	0.45	0.35	0.46
NM_019280	Gap junction membrane channel protein alpha 5	*Gja5*	0.46	0.16	0.28
NM_133293	GATA binding protein 3	*Gata3*	0.47	0.47	0.24

Abbreviations: MMI, 2-mercapto-1-methylimidazole; PTU, 6-propyl-2-thiouracil.